Tu-Pos81

STRUCTURAL ORGANIZATION AND CHANNEL PROPERTIES OF THE MAJOR INTRINSIC PROTEIN OF THE LENS FIBER JUNCTION. N. Lagos, G.R. Ehring, J.E. Hall and G. A. Zampighi. Depts of Physiology and Anatomy, UCLA, Los Angeles CA,90024, Dept. of Physiology and Biophysics UCI, Irvine CA 92717.

We have determined the structural organization of lens junctions in which the major intrinsic protein is a 28 kD polypeptide called MIP. Using monoclonal and polyclonal anti-MIPs we have demonstrated that these junctions are antisymmetric structures composed of tetramers of MIP in a single membrane abutted against an apposed particle-free membrane. Thus a principal characteristic of these junctions is that MIP in them does not form coaxially aligned gap junction-like channels.

Junctional membranes were solubilized with octylglucoside and their protein components separated by HPLC in a strong anion exchange column. Under these conditions MIP eluted in two separate peaks, one of which was demonstrated to be endogenously phosphorylated. Treatment of the junctions before solubilization with alkaline phosphatase eliminated the endogenous phosphorylated peak. Incubation of purified dephosphorylated MIP in the presence of ATP, Mg^{2+}, db-cAMP and protein kinase A resulted in the reappearance of the phosphorylated peak. SDS-PAGE autoradiograms showed that ^{32}P was covalently bound to MIP. See also abstract of Ehring et al. Supported by NIH grants EY05661, EY06075 and EY04110.

Tu-Pos82

DYNAMICAL ENERGY STORAGE IN BIOMOLECULES. Roger E. Clapp, The MITRE Corporation, Bedford, MA 01730.

Many biomolecules use the phosphate group to store energy for immediate use, but the actual energy varies widely from one molecule to another. In cGMP we have shown [Clapp, Biophys. J. 53, 535a (1988)] that the stored energy can be interpreted as an electronic excitation in which a pi-electron hole circulates in a Möbius orbit six bonds in perimeter. We here extend this concept to five other phosphates. The perimeters range from 5 bonds (phosphoenolpyruvate) to 13 bonds (glycerol 3-phosphate); in each case the stored energy, as measured, approximately equals the kinetic energy of the circulating hole, which is proportional to the inverse square of the perimeter. Several non-phosphate transmitter molecules are also examined, including acetylcholine, epinephrine, serotonin, and GABA. Möbius orbits can again be identified, with kinetic energies falling in a plausible range, well above thermal but well below optical. The binding and communication functions of all these biomolecules are likely to involve the electric and magnetic fields associated with the Möbius electronic excitations.

Tu-Pos83

VOLTAGE DEPENDENCE OF GAP JUNCTION CHANNELS IN CELLS STABLY TRANSFECTED WITH CONNEXIN32 (Cx32) cDNA. A.P. Moreno, B. Eghbali, and D.C. Spray, Dept. Neuroscience, A. Einstein Coll. Med., Bronx, N.Y. 10461

We have stably introduced cDNA encoding Cx32 into a human cell line (SKHep1) that is communication-incompetent (Eghbali et al FASEB J. 3: 19 '89), enabling direct study of Cx32 gap junction channels. In parental cells, junctional conductance (g_j) was low or absent (<10 pS in 64/74 cell pairs; in the 10 coupled pairs, g_j was 60-600 pS). In transfected pairs, more than 70% displayed g_j>1 nS, and g_j averaged about 5 nS. Unitary conductances (γ_j) in parental and transfected cells were compared under conditions of low g_j. In control cells where g_j was detectable, γ_j averaged 29±7 pS, and this channel may represent a novel connexin type. In transfected cells a larger channel was expressed, with γ_j 120±25 pS; the small channel seen in control cells was also usually present. Open time of Cx32 channels was markedly voltage dependent. In voltage clamped cell pairs, g_j decreased exponentially with commands of either sign to minimal values (g_{min}) of 0.1 to 0.15 initial g_j (g_{max}). V_0, the voltage at which $(g_{max}-g_{min})=0.5$, was about 25 mV. Polarity reversal experiments, in which a pulse of one polarity sufficient to reduce g_j to low levels preceded a large pulse of opposite polarity, indicate that the Cx32 channel has two series voltage dependent gates, one of which must open before the other gate can close. Cx32 contains no sequence homologous to the S4 domain of nonjunctional voltage-sensitive channels; studies with other connexins and mutant constructs should clarify the location and nature of the voltage sensor(s) on this channel.

Tu-Pos84

DISTINCTIVE TYPES OF GAP JUNCTION CHANNELS CONNECT INDIVIDUAL PAIRS OF WB CELLS. D.C. Spray, M. Chanson, A. P. Moreno, R. Dermietzel, and P. Meda (Spon: R.E. Hirsch). Dept. Neuroscience, A. Einstein Coll. Med., Bronx, N.Y. & CMU, Geneva, Switzerland.

Gap junctions and electrical and dye coupling were investigated in a cell line derived from rat liver (WB cells), that display a phenotype similar to "oval" cells. In freeze fracture replicas, gap junction particles were of distinctive sizes; immunocytology suggests that connexin 43, the cardiac gap junction protein, is expressed in WB cells. An incompletely characterized brain gap junction-associated antigen, MW 34 kDa was also identified at cell interfaces using a specific antibody, whereas no staining was observed using antibodies prepared against other gap junction proteins. Pairs of WB cells were electrically and dye coupled. Under control conditions, coupling between recently dissociated pairs of WB cells was weak or moderate (averaging about 12 nS in 42 cell pairs). Unitary junctional conductances showed three distinctive amplitudes (in CsCl internal solution, about 20-30, 70-80 pS and 90-110 pS, the sum of the other two sizes). Reducing total g_j by a variety of treatments did not produce a pronounced shift toward occupancy of the lower conductance state as would be expected if the uncoupling were favoring occupancy of a channel substate. We conclude that the distinctive unitary conductances represent openings and closures of multiple types of gap junction channels. These channels may correspond to the dual immunoreactivity and to the two particle sizes seen in freeze fracture.

Tu-Pos85

STRUCTURE-FUNCTION ANALYSIS OF CONNEXIN 32 GAP JUNCTION PROTEIN BY DELETION MUTAGENESIS. G. Dahl, R. Werner, E. Levine, C. Rabadan-Diehl. Depts. of Physiology and of Biochemistry University of Miami, Florida 33101.

Carboxyl terminal deletion mutants of the gap junction protein connexin32 were tested in the oocyte cell-cell channel assay. Oocytes expressing one of these mutants (Con 32 D225), lacking 58 carboxyl terminal amino acids, were found to exhibit junctional conductances of the same magnitude as oocytes expressing wildtype connexin32. The deleted segment includes sites that have been proposed to regulate the channels by phosphorylation. The gating properties of the channels formed by Con 32 D225 with respect to transjunctional voltage and cytoplasmic acidification are indistinguishable from those found with wildtype connexin32 channels. This includes a novel pH-dependent voltage gate. Both wild type and con 32 D225 channels are voltage independent at physiological pH but reversibly exhibit a voltage gate upon cytoplasmic acidification. A reverse relationship between pH and voltage dependence exists for the oocyte's endogenous cell-cell channels. [Supported by NSF DCB-8911238.]

Tu-Pos86

SIMILARITY OF CALCIUM DOSE-RESPONSE CURVES FOR OPENING OF CALCIUM-ACTIVATED POTASSIUM CHANNELS, FOR MEMBRANE DEPOLARIZATION, AND FOR SECRETION IN PARATHYROID CELLS. Gerald Ehrenstein, Min Jia, and Susan Pocotte, Laboratory of Biophysics, NINDS, NIH, Bethesda, MD 20892.

Parathyroid cells respond to calcium in a manner that is quite different from the response of other cells. In particular, three different cellular properties exhibit a biphasic dependence on calcium concentration. These properties are the open probability of calcium-activated potassium channels, the membrane potential, and hormonal secretion. Furthermore, the peak for each of these properties corresponds to about the same value of internal calcium concentration (200 nM). It is straightforward to relate membrane potential to the opening of the calcium-activated potassium channels. Is hormonal secretion also related to the opening of calcium-activated potassium channels? We present a model for secretion in general that is based on the opening of these channels in secretory vesicles.

Tu-Pos87

DEVELOPMENTAL CHANGES IN VOLTAGE-SENSITIVITY OF GAP JUNCTIONAL CONDUCTANCE. By Richard D. Veenstra, Dept. of Pharmacology, SUNY/HSC, Syracuse, NY 13210.

The dependence of macroscopic gap junctional conductance ($G_j = I_j/V_j$) on trans-junctional voltage ($V_j = V_2 - V_1$) was examined in paired myocytes isolated from 4-day or 14-day embryonic chick ventricles and cultured for 1 day in vitro using the double whole cell patch clamp technique. Instantaneous I_j-V_j relationships for 4-day and 14-day cell pairs were linear over the entire voltage range of ±100 mV, indicating that the gap junction channels initially behave as a simple ohmic resistor. However, I_j undergoes a time- and V_j-dependent decline at all voltages examined in 4-day heart. Similar inactivation of I_j is not observed in 14-day heart until V_j exceeds ±30 mV. The normalized steady-state G_j-V_j curves for 4- and 14-day heart (n = 8 for each curve) reveal significant differences in G_j at low (≤ ±40 mV) and high (≥ ±80 mV) V_j values ($p < .05$, unpaired t-test). The steady-state G_j curve can be adequately described by a two-state Boltzmann equation previously used for other voltage-dependent gap junctions. From the theoretical fit of the steady-state G_j curves for 4- and 14-day heart, the minimum G_j was 0.18 and 0.28; the half-inactivation voltage was 39 mV and 49 mV; and the effective gating charge was 1.5 and 2.0 electrons respectively for 4-day and 14-day cell pairs. These values reflect a gradual loss of voltage-sensitivity during cardiac development. This work is currently being extended to 18-day heart cell pairs. This study was supported by NIH HL-42220 and National AHA 880708.

Tu-Pos88

SINGLE AND MULTICHANNEL RECORDINGS FROM GAP JUNCTION MEMBRANES.

K. Manivannan, S. V. Ramanan, R. T. Mathias and P. R. Brink.
HSC, SUNY at Stony Brook, NY 11794.

Single and multiple gap junction channel recordings are obtained using the patch clamp technique. Experiments are done with excised patches from the septal membrane of the median giant axon of the earthworm and the records vary from 5 to 30 minutes. The unitary conductance of single channel records is 90-110 pS. However, the conductance levels of multichannel records are not usually fit by integer multiples of a unitary conductance. The observed probabilities of the various conductance levels can sometimes be fit by a binomial distribution assuming independent identical channels; however, in many instances, at least two different independent probabilities are required. We have considered several possible explanations. The channels in the patch could be: 1) independent and not identical; 2) identical but they gate co-operatively; 3) structurally identical but functionally different due to ligand binding.

Grants HL36075, EY06391, GM24905, HL31299

Tu-Pos89

QUANTITIVE MEASUREMENT OF JUNCTIONAL CONDUCTANCE AND DYE PERMEABILITY IN BLASTOMERES OF SQUID AND TUNICATE.

C.D. Leidigh and M.V.L. Bennett. Marine Biological Laboratory, Woods Hole, MA 02543, Brown University, Providence, RI 02912 and Albert Einstein College of Medicine, Bronx, NY 10461.

Early blastomeres of squid, Loligo, and tunicate, Phalusia, are electrically and dye coupled. To correlate total permeability, P_j, and junctional conductance, g_j, one of a pair of cells was rapidly injected with a mixture of 5 and 6 carboxyfluorescein, and dye movement was followed to near equilibration with quantitive measurement of fluorescent intensity by means of an image analysis system. The two cells were then each penetrated with two electrodes and g_j measured under voltage clamp. Dye movement was reasonably exponential, if fluorescence excitation was minimized; thus binding and bleaching as well as leakage were negligible. Time constants were generally hundreds of seconds. Permeability was calculated as $V_1 V_2/((V_1 + V_2)\tau)$, where V_1 and V_2 are cell volumes and τ is the time constant of equilibration. Mean P_j/g_j ratios were 1.2×10^{-4} for squid and 4.6×10^{-4} for the tunicate. The squid value is comparable to that for tetrabutylammonium ions (unpublished data with V.K Verselis, D.C. Spray and R.L. White); although the dye molecule is larger, it has a negative charge which may affect its permeation. The somewhat higher P_j/g_j ratio for the tunicate suggests that the voltage gating mechanism present in these gap junctions does not impede chemical fluxes when the channels are open.

Tu-Pos90

Ca CURRENTS, Ca_i CHANGES AND EXOCYTOSIS IN SINGLE ENDORPHIN/αMSH-SECRETING RAT PITUITARY CELLS.

P.Thomas, A.Surprenant* & W. Almers, Dept. Physiol., U.Wash. Seattle WA; *Vollum Inst. (OHSU), Portland, OR.

To see how calcium currents (I_{Ca}) influence secretion, we recorded cytosolic [Ca] (Ca_i, fura-2), I_{Ca} and capacitance (C, a measure of cell surface area) in single melanotrophs in primary (1-20d) culture. Peak I_{Ca} (10 mV, 5mM $[Ca]_o$) varied widely (21°C: <5pA to 190pA: mean 80±20pA, C=5±.5 pF, n=8) and increased with temperature (32°C: 50-500pA, mean 290±30pA, C=4.4±.2 pF, n=10). At rest, Ca_i= 120±20 nM (n=36, 10 mM $[Ca]_o$). Single 200ms steps to 20 mV raised Ca_i in proportion to I_{Ca} (by 15±2 nM*pF/pA, n=10). Trains of such steps increased C (caused exocytosis) only if they raised Ca_i beyond 400nM. Even for Ca_i >400nM, only half of the cells exocytosed. Peak Ca_i for cells that exocytosed (890±180nM, n=7) and those that did not (690±80 nM, n=8) differed little. Probably other factors besides Ca_i control secretion. When Ca_i was controlled through the pipette, C increased by 21±4%, n=8, in 6 min when Ca_i ≈1 μM (9.5mM Ca/10mM EGTA) but not (by 0±3%, n=6) when Ca_i 20 nM (0Ca/10mM EGTA in the pipette). Supported by AR-17803, NS-07097.

Tu-Pos91

CELL-TO-CELL PERMEABILITY IN DISSOCIATED EMBRYONIC CHICKEN LENSES.

A.G. Miller, J.E. Hall, G.A. Zampighi, Dept. of Physiology and Biophysics, University of California at Irvine, Irvine, Ca 92717, Dept. of Anatomy, Jerry Lewis Neuromuscular Research Center, University of California at Los Angeles, Los Angeles Ca 90024.

Embryonic chicken lenses were removed from the eye and enzymatically digested with trypsin into single cells, cell pairs, and cell clusters. Using the patch clamp technique, cell coupling was monitored both electrically and with dye. Simultaneous injection of lucifer yellow (MW=457) and a rhodamine labelled dextran (MW=10,000) showed that lucifer yellow spread to adjacent cells within minutes, whereas no rhodamine labelled dextran was observed in adjacent cells 15 minutes after injection. Whole cell patch clamp measurements made on one cell of a coupled pair, while simultaneously monitoring spread of lucifer yellow, revealed little voltage-dependent current over the range of -60mv to +40mv. The input resistance of these cell pairs ranged from 1 to 6 G-Ohms. Double patch clamp measurements made on pairs of cells, with both cells clamped in whole cell mode, showed junctional conductances ranging from about 15 nS to greater than 30 nS. The electrical coupling decreased as a function of time in all experiments and in some cases single cell to cell channels with unit conductances ranging from 200-300 pS were observed. Freeze fracture on these cells revealed the presence of gap junctions. Supported by NIH grants EY05661, EY06075 and EY04110.

Tu-Pos92

EXPRESSION OF CONNEXIN43 FROM VASCULAR SMOOTH MUSCLE IN A MOUSE EMBRYO MODEL.

Milton L. Pressler, Elizabeth Critser* and Joseph A. Lash. Department of Medicine and the Krannert Institute of Cardiology, Indiana University School of Medicine, and *Methodist Hospital, Indianapolis, IN.

Gap junctional proteins (connexins) are thought to be the molecular basis for cell-cell communication in heart, liver, and lens. However, little is known regarding regulation of cellular coupling in smooth muscle, such as that which occurs during segmental contraction of blood vessels. We have recently isolated a cDNA from vascular smooth muscle (VSM) encoding a gap junctional protein. To investigate the functional role of VSM connexin43, we took advantage of the fact that B6D2F1 mouse embryonic cells are not coupled until the 4-cell stage. We verified this by intracellular injection of Lucifer Yellow: 0/24 2-cell, 12/17 4-cell, and 17/18 8-cell embryos were dye-coupled. *In vitro* transcribed VSM connexin43 mRNA (0.3-1.0 pg) was microinjected into fertilized eggs. After cell division, 57% (19 of 33) of the 2-cell embryos showed intercellular transfer of dye within 15 min. Initial studies of the fate of microinjected embryos shows no developmental effects of connexin43 up to the blastocyst stage. Our results demonstrate the functional activity of a VSM connexin and suggest that early mouse embryos may be useful as a mammalian expression system for study of cell-cell coupling.

Tu-Pos93

ION CHANNELS FORMED IN SINGLE BILAYERS BY THE GAP JUNCTION PROTEIN CONNEXIN32.

A.L. Harris[1], C. Bevans[1], A. Walter[2], D. Paul[3], D.A. Goodenough[3] & J. Zimmerberg[4]. [1]Dept. Biophys., Johns Hopkins Univ., [2]Dept. Physiol. & Biophys., Wright State Univ., [3]Dept. Anat. & Cell Biol., Harvard Med. Sch., [4]Phys. Sci. Lab., DCRT & Lab. Biochem. & Metab., NIDDK, NIH.

Connexin32 (Cx32) is the major channel-forming protein of liver gap junctions. We show that Cx32 forms ion channels in single artificial membranes by (1) incorporating junctional protein into liposomes, (2) selecting liposomes on the basis of permeability to a large molecule, and (3) identifying the protein responsible for the permeability with a monoclonal antibody. Liposomes were formed in the presence of protein solubilized from isolated gap junctions, and then fractionated into sucrose-permeable (S-P) and sucrose-impermeable (S-IMP) populations. Proteins in each population were analyzed by blots probed with anti-Cx32 monoclonal antibody and by total protein stain. Cx32 was specifically enriched in the S-P liposomes, relative to its proteolytic fragment, and was almost absent in the S-IMP liposomes. In the S-P population, there was sufficient Cx32 per liposome to compose several connexons, and no detectable non-Cx32 protein. We conclude that in liposomes, Cx32 forms sucrose-permeable channels that are open at zero membrane voltage. Planar bilayer studies show that the channels have properties consistent with being single connexons (large conductance, weak charge selectivity, asymmetric voltage dependence). Open probability shows a first-order dependence on voltage. Supported by NIH GM36044 to ALH, GM37751 to DP, GM18974 to DAG and BRSG S07RR07041 to Johns Hopkins Univ.

Tu-Pos94

MODULATION OF GAP JUNCTION CONDUCTANCE BY TRANSCELLULAR ELECTRICAL FIELDS.

H.J. Jongsma, R. Wilders, M.B. Rook. Dept. of Physiology, Univ. of Amsterdam, 1105 AZ Amsterdam, The Netherlands.

The total gap junctional conductance of pairs of neonatal rat heart cells is relatively high and appears to be voltage independent. The single channel conductance on the other hand exhibits a clearcut voltage dependence based on a decrease of the mean open time of the channels with increasing transcellular voltage. Our hypothesis is that this difference in behaviour is caused by a decrease in the electrical field and consequently the transjunctional voltage across the gap junctions when the number of channels comprised in it increases. To test this hypothesis we constructed a simple model based on the calculation of the electrical field at any point in a system of two cells connected by idealized gap junction channels in a hexagonal array. The resulting partial diffential equation of Laplace was solved using a finite difference representation of this equation in polar coördinates. The results show that a junction consisting of one channel senses 98 % of the applied voltage. With increasing numbers of channels this figure decreases: e.g. a junction consisting of 500 channels senses only 65 % of the applied voltage. When a more realistic geometry is used the relation is even steeper. Thus it seems feasible that the absence of voltage dependence in larger gap junctions simply is the result of a considerable voltage drop across the cytoplasmic resistance present between the electrodes and the gap junction.

Supported by NWO grant no.810-406-151

Tu-Pos95

GAP JUNCTION FUNCTION IN NEONATAL RAT CARDIAC MYOCYTES IS ALTERED BY EXPOSURE TO A FREE RADICAL GENERATING SYSTEM.

Kenneth D. Massey and Janis M. Burt. University of Arizona, Physiology Department Tucson, Arizona 85724

Intercellular communication between myocardial cells occurs via gap junctions. Gating of these channels is affected by intracellular calcium concentration, pH, cAMP and a variety of lipophillic substances. Closure of gap junction channels results in interruption of communication between adjoining myocardial cells may be related to the occurrence of cardiac dysrhythmias. Free radical compounds, whose action may result in dysrhythmias, are formed during ischemia and reperfusion. The relationship between free radicals and alterations in gap junction function is being investigated in a neonatal rat cardiac myocyte model with lucifer yellow dye-coupling and dual whole-cell voltage clamp techniques. The cells were exposed to a xanthine oxidase-catalyzed free radical generating system capable of producing both superoxide and hydroxyl radicals. Five minutes of superfusion with the radical generating system resulted in complete loss of junctional permeability. Returning to non-radical producing perfusate was accompanied by the return of junctional permeability in approximately 30% of the cell pairs analyzed. Work is continuing to determine the mechanism underlying these observations. Supported by: NS07309, HL07249 and HL31008.

Tu-Pos96

ANTIARRHYTHMIC DRUGS HAVE A MINOR EFFECT ON GAP JUNCTION CONDUCTANCE.

Lisa K. Moore and Janis M. Burt. Dept. of Physiology, University of Arizona, Tucson, Arizona.

In recent years dysrhythmia generation and re-entrant phenomena in myocardium has been linked to changes in gap junction conduction. In addition many lipid soluble substances of appropriate chain length and structure affect junctional communication. The ability of Class I - V antiarrythmics (Mayo Clin Proc 54:531, 1979) to change propagation speed, excitability of the myocardium, and stabilize membrane potential, thereby preventing re-entry rhythms and dysrhythmias has been well documented. This is thought to occur primarily through regulation or blockade of various ion channels. The ability of lidocaine, procainamide, verapamil and amiodarone to influence gap junction function in neonatal myocytes in tissue culture is evaluated in this study. Cell pairs were dual whole-cell voltage clamped and measurements of junctional conductance before and during application of the drug were recorded. Results are reported as maximum percent change (± SEM) in conductance from control conditions. Lidocaine (1mM, n=8) reduced conductance by 10.8 ± 8.2%. Procainamide (1mM, n=5) reduced conductance by 12 ± 3.95%. Amiodarone (1uM and 5uM, n=3 for each) reduced conductance by 6 ± 3.75%. Verapamil (1mM, n=2) reduced conductance by 10%. These results indicate the role of gap junctions in the mechanism of action of antiarrhythmics is minor. Supported by: NS07309, HL07249, HL31008.

Tu-Pos97

MITOGENIC STIMULATION OF HUMAN T CELLS BY SOLID TUMOR LINES MEDIATED BY SECRETED PROTEINS. Beverly S. Packard and Akira Komoriya. DCB, CBER, FDA, Bethesda, MD. 20892.

Tumor infiltrating lymphocytes (TILs) are populations of T cells that have been grown directly from tumors in the presence of interleukin-2 (IL-2). TILs used in this study were from human melanoma tumors and continue to respond to the IL-2 mitogenic signal. However, at least three TIL lines can be stimulated to grow in culture in the absence of IL-2 if serum-free supernatants from either of two human solid tumor cell lines are added. In contrast to the classical IL-2-induced sigmoidal mitogenic dose-response curve which plateaus at *ca.* 48 hours, tumor cell supernatants induce a maximal rate of thymidine incorporation by 12 hours; furthermore, in the presence of these serum-free media lymphocytes aggregate into clusters (>50 cells each) which results in inhibition of their motility. This latter property is in sharp contrast to the highly motile behavior observed by IL-2-stimulated TILs and lymphocytes in general; it may represent a heretofore unrecognized mechanism of immunoregulation.

Tu-Pos98

COMPLEX VOLTAGE DEPENDENCE OF GAP JUNCTIONAL CONDUCTANCE IN DROSOPHILA

V.K. Verselis, M.V.L. Bennett and T.A. Bargiello, Dept. of Neuroscience, Albert Einstein College of Medicine, Bronx NY 10461.

Gap junctional conductance, g_j, in salivary glands of *Drosophila melanogaster* third instar larvae is affected by voltages applied between the cells, *i.e.* transjunctional voltages, V_j, and those applied between the cytoplasm and the exterior, inside-outside voltages, V_{i-o}. Action of V_{i-o} is polarity dependent such that g_j increases to a maximum on hyperpolarization and decreases to near zero on depolarization. Either polarity of V_j substantially reduces g_j. V_{i-o} sensitivity is greater than V_j sensitivity, but the changes in g_j are slower. Rate constants for transitions between steady-state g_j's for equal steps to both cells, *i.e.* V_j=0, V_{i-o} variable, exhibit simple exponential dependence on voltage; the rate constant for closure is 4-fold more sensitive than the opening rate. Changes in g_j caused by voltage steps in one cell exhibit complex kinetics consistent with the combined actions of V_j and V_{i-o}. The two voltage dependencies interact such that conductance decreases caused by V_j are faster and proportionally greater when the holding potential in the two cells (V_{i-o}) is more positive. In salivary glands of *Drosophila virilis*, V_{i-o} dependence is conserved, but V_j dependence is nearly absent suggesting that, although the gating domains interact, they may be distinct sites within the channel. The data are consistent with the view that gap junction channels are mirror symmetric around the center of the gap and that each hemichannel contains voltage gating elements.

Tu-Pos99

A NEW PROBE FOR DETECTING CALCIUM SIGNALLING VIA CALMODULIN.

Klaus M. Hahn, D. Lansing Taylor, Alan S. Waggoner. Center for Fluorescence Research in the Biomedical Sciences, Biology Department, Carnegie Mellon University, Pittsburgh, Pennsylvania.

Structure-activity studies enabled the design and synthesis of a novel fluorophore showing calcium dependent binding to calmodulin. The fluorophore was covalently attached to calmodulin, creating a calcium sensitive calmodulin analog. An excitation ratio taken at 532 and 605 nm, with emission at 623 nm, showed a sigmoidal dependance on calcium concentration, with a half maximal value at 0.5-1 μM Ca and 3 fold total change. The concentration dependence of the adduct's myosin light chain kinase activation paralleled that of unaltered calmodulin. The long excitation and emission wavelengths of the adduct, and the strong dependence of its excitation ratio on calcium concentrations in the physiological range suit it well for use as a probe of calmodulin dependent calcium signalling.

Tu-Pos100

INTRACELLULAR PROTON CONCENTRATION DEPENDENCE OF Na^+/H^+ EXCHANGE FOLLOWS MICHAELIS MENTEN KINETICS IN HL60 CELLS.

D. Restrepo, D.S. Cho and M.J. Kron. Monell Chemical Senses Center, Philadelphia, PA.

The pH_i dependence of Na/H exchange was studied in suspensions of HL60 cells by assaying rates of alkalinization at different starting pH_i using the fluorescent dye BCECF. Because it was found that Na/H exchange saturated only at pH_i values lower than 6.0, the dye was carefully calibrated in situ in the pH range from 5.0 to 7.5 using nigericin and high extracellular potassium (Biochemistry 18:2210-8,1979) and by carefully quantitating extracellular BCECF (ecf BCECF). Differences between pH_o and pH_i caused by differences between $[K_i]$ and $[K_o]$ during the nigericin-high potassium calibration were carefully evaluated and found to be small, but significant. Using in situ calibration and taking on account fluorescence from ecf BCECF, it was found that the dependence of Na/H exchange on $[H_i]$ follows Michaeilan kinetics. Failure to calibrate the dye in situ and/or to take on account ecf BCECF results in a sigmoid dependence of Na/H exchange on $[H_i]$.

Tu-Pos101

DIFFERENTIAL INHIBITION AND ACTIVATION OF PROTEIN KINASE C ISOZYMES BY SURAMIN.

C.W. Mahoney(1), A. Azzi(2), & K-P. Huang(1); (1) Endocrinol. & Reprod. Research Branch, NICHD, NIH, Bethesda, MD 20892; (2) Institute of Biochem. & Mol. Biol., Univ. of Bern, Bern, Switzerland.

Suramin, an HIV reverse transcriptase agent, inhibited types I, II, and III protein kinase C (PKC) in a type-dependent manner (I>II=III; IC50s≈30-60 μM). M-kinase, the constitutively active fragment of PKC, and autophosphorylation of holo-PKC were similarly inhibited suggesting that inhibition is through the active site within the catalytic domain. Kinetic competition experiments indicate that suramin competitively inhibits activity with respect to ATP. In the case of histone IIIS as substrate the mechanism of inhibition can also be by inactivation of the substrate. On the other hand, in the presence of calcium and absence of lipid, suramin (10-40 μM)(I>III>II) was able to activate (~200-400%) and at higher concentrations inhibited kinase activity. It appears that suramin, a hydrophobic hexaanion, can act as a negatively charged phospholipid analog in activating PKC in the presence of calcium and absence of lipid. Suramin inhibited cAMP dependent protein kinase much less potently (IC50 = 656 μM) than PKC. These data suggest that suramin may inhibit HIV infection as well as HIV replication (cf. Fields, A.P. et al.(1988) Nature 333, 278-280).

Tu-Pos102

MITOCHONDRIAL DEPOLARIZATION DOES NOT LEAD TO INTRACELLULAR CALCIUM RELEASE IN CULTURED RAT HEPATOCYTES EXPOSED TO $HgCl_2$ OR UNCOUPLER.

Anna-Liisa Nieminen, Toru Kawanishi, Brian Herman and John J. Lemasters, Department of Cell Biology & Anatomy, University of North Carolina, Chapel Hill, NC 27599.

Hg^{2+} binds with high affinity to protein and non-protein thiols. Using multiparameter digitized video microscopy (MDVM) of single cultured rat hepatocytes and the fluorescent probes monochlorobimane and monobromobimane, protein and non-protein thiol oxidation was virtually 100% complete after 90 seconds exposure to 50 μM $HgCl_2$. Within 1 minute following, mitochondria abruptly became depolarized as indicated by the redistribution of rhodamine 123 into the cytosol. No increase of cytosolic free Ca^{2+} measured by ratio imaging of Fura-2 fluorescence accompanied mitochondrial depolarization although free Ca^{2+} subsequently increased 3-4 minutes later. An identical sequence occurred in low Ca^{2+} (<2 μM) medium but without a late increase of Ca^{2+}. 2 μM CCCP, an uncoupler, was also added to depolarize mitochondria. No increase of free Ca^{2+} followed for several minutes in normal or ATP-depleted cells. In conclusion, no significant gradient of Ca^{2+} appears to exist between the cytosol and the mitochondrial matrix in cultured hepatocytes.

Tu-Pos103

TENIDAP AS A PHARMACOLOGICAL TOOL IN THE STUDY OF CALCIUM MOVEMENTS IN MAST CELLS

Patricia L. Cleveland, Henry J. Showell†, and Clare Fewtrell, *Department of Pharmacology, Cornell University, Ithaca, NY and †Department of Immunology and Infectious Diseases, Pfizer Central Research, Groton, CT.*

The antigen-induced cross-linking of immunoglobulin E receptors on the surface of tumor mast cells leads to a secretory response that is preceded by an increase in intracellular Ca^{2+}. Both release of Ca^{2+} from intracellular stores and influx across the plasma membrane contribute to the changes in intracellular Ca^{2+}. The new anti-inflammatory agent tenidap (1989. *Arth. Rheum.* 32:S148) has been shown to inhibit secretion from tumor mast cells and in this study we have examined its effects on Ca^{2+} handling by these cells. In antigen-stimulated cells, tenidap inhibits ^{45}Ca influx and secretion of ^{3}H-serotonin with an IC_{50} of ~10 μM. In addition, the compound alone causes efflux of preloaded ^{45}Ca from unstimulated cells, by a mechanism that appears to be independent of phosphoinositide breakdown. We conclude that tenidap both inhibits Ca^{2+} influx through the voltage insensitive Ca^{2+} channel or pathway and releases Ca^{2+} from intracellular stores, and that the effects of the compound on secretion are due to effects on Ca^{2+} handling. These results suggest that tenidap will prove useful in studying Ca^{2+} movements in nonexcitable cells. The possibility that tenidap is a selective inhibitor of voltage-insensitive Ca^{2+} channels in these cells is particularly exciting.

Tu-Pos104

AGONIST-STIMULATED Ca^{2+} AND Ba^{2+} FLUXES IN CULTURED VASCULAR ENDOTHELIAL CELLS. William P. Schilling and Lekha Rajan. Baylor College of Medicine, Houston, TX.

Previous fura-2 studies suggested that the bradykinin (BK)-stimulated Ca^{2+} influx pathway of bovine aortic endothelial cells (BAECs) allows both Ca^{2+} and Ba^{2+} to enter the cell, but that Ba^{2+} is not sequestered by intracellular mechanisms. In the present study, influx of $^{45}Ca^{2+}$ and $^{133}Ba^{2+}$ was measured in the absence and presence of BK. BK stimulated the influx of both isotopes in a dose-dependent manner with an apparent ED_{50} of 0.3 nM. To determine if Ba^{2+} enters, and is released from, the IP_3-sensitive Ca^{2+} pool, fura-2-loaded cells were 1) depleted of Ca^{2+}, 2) allowed to re-load with either Ca^{2+} or Ba^{2+}, and 3) subsequently challenged in the presence of La^{3+} with the agonist, ATP. ATP produced a large change in $[Ca^{2+}]_i$ with little change in $[Ba^{2+}]_i$. This suggests that Ba^{2+} is not concentrated in or released from the IP_3-sensitive Ca^{2+} store. To further test this hypothesis, BAECs, equilibrated with tracer amounts of $^{45}Ca^{2+}$ or $^{133}Ba^{2+}$ either in the absence or presence of BK, were employed for the measurement of BK-stimulated isotope efflux. Loading the cells with $^{45}Ca^{2+}$ in the presence of agonist had no effect on the amount of isotope accumulated by the cells or on the subsequent efflux which was stimulated 27-fold by the addition of BK. $^{133}Ba^{2+}$ efflux was stimulated only 3-fold by BK. However, loading of the cells with $^{133}Ba^{2+}$ in the presence of BK resulted in a 1.3-fold increase in $^{133}Ba^{2+}$ associated with the cells at equilibrium and a partial inhibition of the BK-stimulated $^{133}Ba^{2+}$ efflux. These results suggest that there is a compartment within the BAECs that is accessible to Ba^{2+} only in the presence of BK and that the presence of Ba^{2+} in this compartment may inhibit BK-stimulated Ca^{2+}-release from internal stores. Thus, while Ba^{2+} apparently is not actively accumulated within the internal store, it may gain access to this compartment via the IP_3-sensitive release pathway.

Tu-Pos105

GLUCOCORTICOIDS CHANGE THE FORMS OF ADRENOCORTICOTROPHIN SECRETED BY ANTERIOR PITUITARY CORTICOTROPHS

JC Normant*, AM Gurney† and B Gillham* (Intro. by N. Mulrine) Depts. of Pharmacology† and Biochemistry*, UMDS, St Thomas's Hospital, London, UK.

Glucocorticoids inhibit the secretion of adrenocorticotrophin (ACTH) from cultured rat anterior pituitary cells. Reversed-phase HPLC analysis (with heptafluorobutyric acid (HFBA) as ion pairer) of the secreted peptides, revealed that this inhibition was associated with changes in the molecular forms of ACTH-immunoreactivity released. Two main forms were resolved, and one could be converted to the other by treatment with alkaline phosphatase prior to HPLC analysis. It is probable, therefore, that they represented phosphorylated (ACTH-p) and non-phosphorylated (ACTH-n) forms of ACTH, which have been described previously. Brief (20 min) exposure to dexamethasone (DEX; 100nM) changed the ratio of ACTH-n to ACTH-p secreted in response to CRF (10 nM, 15 min), from 2.53 ± 0.39 (mean ± s.e.m.; n=5) to 0.83 ± 0.19 (n=4); significant at $P<0.01$. A further steroid-induced modification of ACTH was revealed after dephosphorylation, when the peptide released in the presence of DEX was found to be more hydrophobic (under the HFBA conditions employed) and possessed 4-5 times less adrenocorticotrophic bioactivity than the ACTH released in its absence. The peptide also had a reduced N-terminal immunoreactivity, suggesting a modification at this end of the molecule. These modifications of the ACTH molecule may well contribute to the depression of bioactivity released in the presence of glucocorticoids.

Tu-Pos106

IONOPHORES INCREASE INTRACELLULAR CALCIUM IN THE ABSENCE OF EXTRACELLULAR CALCIUM.

A. H. Lansley, E. R. Dirksen and M. J. Sanderson. Department of Anatomy and Cell Biology, UCLA School of Medicine, University of California, Los Angeles, CA 90024.

The calcium ionophores ionomycin and A23187 were applied to respiratory tract ciliated cells in culture in the absence of extracellular calcium in an attempt to reduce intracellular calcium ($[Ca^{2+}]_i$). Under these conditions 1 μM ionomycin induced a rapid increase in ciliary beat frequency (CBF). A slower and smaller increase in CBF was observed with 1 μM A23187. Since CBF of ciliated cells is elevated by Ca^{2+}, we suggest that these ionophores are acting to increase $[Ca^{2+}]_i$. This hypothesis was confirmed by fura-2 ratio imaging; in the absence of extracellular Ca^{2+} cells showed an immediate increase of $[Ca^{2+}]_i$ when exposed to 1 μM ionomycin. Exposure to 1 μM A23187 illicited a similar but smaller increase of $[Ca^{2+}]_i$. CBF and $[Ca^{2+}]_i$ were restored to pre-application values after approximately 5 minutes and after 10 minutes $[Ca^{2+}]_i$ was seen to diminish as expected. In addition to increasing cell membrane permeability to Ca^{2+}, these ionophores act initially to release Ca^{2+} from intracellular stores of intact cells in a manner not unlike that of IP_3. Supported by the Smokeless Tobacco Research Council, Inc. and the Cystic Fibrosis Foundation.

Tu-Pos107

ADENOSINE DEAMINASE COMPLEXING PROTEIN: A MALIGNANT-TRANSFORMATION MARKER IN CHICK EMBRYO FIBROBLASTS

Yoav Roth, Nurith Porat, Yoav Sharoni and Abraham H. Parola*, Department of Chemistry Ben-Gurion Universityof the Negev Beer-Sheva, Israel 84 150

Adenosine deaminase complexing protein (ADCP) is present in considerable quantities in certain human tissues yet, it is absent or decreased in the cancers orignating from them. A similar qualitative trend was recently reported by us with chick embryo fibroblasts (CEF) transformed by Rous sarcoma virus (RSV). Furthermore phase fluorometry revealed that RSV transformation of CEF is associated with a dramatic increase in the rotational dynamics of the membranal adenosine deaminase (ADA) concomitant with a remarkable reduction in its activity. The vertical displacement of ADCP, controlled by lipid-protein interactions was hypothesized as a possible explanation to the observed phenomena. To substantiate this hypothesis we undertook the quantitation of ADCP and the determination of binding affinities between ^{125}I labeled small subunit ADA and ADCP, in normal and transformed CEF. ADCP was determined in intact and hemolized normal and RSV transformed CEF. With intact cells K_d values were determined.

Tu-Pos108

PHOSPHATE INCREASES ATP-RECEPTOR INDUCED [Ca^{2+}] RESPONSES IN CARDIAC MYOCYTES.

Mary Beth De Young and Antonio Scarpa , Department of Physiology and BIophysics, Case Western Reserve University, Cleveland, OH 44106.

A cardiac ATP receptor has been shown to increase Ca^{2+} influx and SR Ca^{2+} release in fura2-loaded adult rat ventricular myocytes. Although extracellular phosphate (Pi) decreases medium free [Ca^{2+}], 11.2 mM extracellular Pi increased both the transient and sustained phases of the cytosolic [Ca^{2+}] response to ATP. The increased transient phase is probably due to increased releasable intracellular Ca^{2+} stores. The increase in sustained cytosolic [Ca^{2+}] was dominant in 11.2 mM extracellular Pi, with [Ca^{2+}] in the μM range compared to 15 $\pm$ 4 nM (mean $\pm$ SE, n=5) with 1.2 mM Pi. Cell hypercontraction and lysis were observed following ATP stimulation in high Pi. KCl stimulated [Ca^{2+}] changes were not similarly Pi dependent. The increase in the secondary phase of the response to ATP was dependent on both Na^+ and Ca^{2+}, suggesting a role for Na^+/Ca^{2+} exchange. The strong Pi dependence suggests that ATP-induced Na^+/Pi cotransport provides the Na^+ influx required to drive Ca^{2+} inward through the Na^+/Ca^{2+} exchanger. (Supported by NIH grants HL 18707 and HL 07502).

Tu-Pos109

CALCIUM SIGNALLING IN HEPATOCYTES: A MICRO-INJECTION STUDY. *Carl A. Hansen, Suresh K. Joseph, Ivo Rogulja, John R. Williamson. Dept. Biochem & Biophys. Univ. of Penn School of Medicine, Philadelphia, PA 19104.*

In fura2 loaded hepatocytes, the agonist induced Ca2+ transient consisted of a variable latency period (sec), a phase of rapid increase due to release of Ca2+ from internal stores and then a period of elevated Ca2+ that was dependent on external Ca2+. Microinjection of GTPγS (~1μM) induced a Ca2+ transient with similar features. Injection of Ins(1,4,5)P_3 (~0.5μM) induced a rapid increase in cytosolic Ca2+ within 200 msec which then returned to basal levels. These data indicated that the latency period was related to the rate of phospholipase C activation by either the activated receptor or G-protein. Injection of Ins (1,4,5)thioS (~0.5μM), a nonhydrolyzable analogue of Ins(1,4,5)P_3, resulted in a rapid rise in Ca2+ similar to that induced by Ins(1,4,5)P_3, but the cytosolic Ca2+ remained elevated. Upon removal of extracellular Ca2+, however, the cytosolic Ca2+ returned towards basal levels, suggesting that Ins(1,4,5)thioS had stimulated Ca2+ entry. These data are consistant with the capacitative model for stimulation of Ca2+ entry. (Supported by AHA grant # 891060).

Tu-Pos110

Ca2+-INDUCED CONFORMATIONAL CHANGES AND LOCATION OF Ca2+-TRANSPORT SITES IN SARCOPLASMIC RETICULUM Ca2+-ATPase AS DETECTED BY THE USE OF PROTEOLYTIC ENZYME (V8). M. le Maire*, S. Lund**, A. Viel*, P. Champeil*** and J.V. Møller**.*C.G.M., C.N.R.S., 91198 Gif-sur-Yvette Cédex, France. **Inst. Med. Bioch., Univ. Aarhus 8000 Aarhus C, Danmark.***URA CNRS 219, Dépt. de Biologie, C.E.N. Saclay, 91191 Gif-sur-Yvette Cédex, France.

Treatment of SR Ca2+-ATPase with V8 protease produced appreciable amounts of a fragment (Mr=85000, p85) in the presence of Ca2+ (E1 conformation of the enzyme), but not in EGTA (E2). p85 was formed as a carboxyterminal cleavage product of Ca2+-ATPase by a split of the peptide bond between Glu231 and Ileu232. Other conformation-dependent V8 splits were localized to the "hinge" region, between the middle and C-terminal one-third of the Ca2+-ATPase polypeptide chain. Representative split products in this region (p48, p31) were identified as N-terminal and C-terminal cleavage products of p85. Binding of Ca2+ to V8 and tryptic fragments of Ca2+-ATPase was studied on the basis of Ca2+ induced changes in electrophoretic mobility and 45Ca2+ autoradiography after transfer of peptides to Immobilon membranes. These data indicate binding by the N-terminal 1-198 amino acid residues (corresponding to the tryptic A2 fragment) and the C-terminal 715-1001 amino acid residues (corresponding to p31). By contrast the central part of Ca2+-ATPase is devoid of Ca2+ binding. These results concerning the Ca2+ translocation sites will be discussed and compared with recent data obtained by directed mutagenesis.

Tu-Pos111

DIFFERENTIAL EFFECTS OF H^+-ATPase INHIBITORS ON INTRACELLULAR pH (pH^{in}). *R. Martinez-Zaguilan & R.J. Gillies (Intr. by D. O'Brien).* Dept. Biochem., U. Ariz.; Tucson AZ 85724. In culture, pH^{in} does not change with stimulation, so it is not a proliferative signal *in vitro*[1]. 3T3 cells transfected with yeast H^+-ATPase (RN1a cells) are tumorigenic. We have measured the pH^{in} in these cells *vis a vis* normal 3T3 cells, and the data suggests that pH^{in} might be important to tumorigenicity *in vivo*. We have also tested the effect of H^+-ATPases inhibitors on pH^{in} in non-tumorigenic and tumorigenic cells. Both NEM and fusidic acid acidify pH^{in} in EAT, RN1a and CHO cells, with different ED_{50} for each cell type. Suramin decreases pH^{in} only in RN1a cells. No specific effects were seen in 3T3 cells. Therefore, these drugs differentially affect pH^{in} regulation in non-tumorigenic and tumorigenic cells. (R01 GM43046-01). [1]Gillies R.J. et.al. J. Biol. Chem. (submitted) [2]Perona R and Serrano R. Nature 334: 438, 1988.

Tu-Pos112

INOSITOL PHOSPHATE SIGNALLING MECHANISM AND NaCl(K) COTRANSPORT ACTIVATION IN AIRWAY EPITHELIAL CELLS (AEC). Carole M. Liedtke. Departments of Pediatrics and Physiology & Biophysics, Case Western Reserve University, Cleveland, OH 44106.

NaCl(K) cotransport is thought to provide intracellular Cl for secretion in AEC. In rabbit and human AEC, NaCl(K) cotransport is quiescent until activated by α-adrenergic agonists, requires intracellular, but not medium, Ca and is stimulated by Ca-ionophore ionomycin. The role of Ca in cotransporter activation is explored by investigating the link between Ca and α-adrenergic receptors. A kinetic analysis of aqueous and lipid components of an IP signalling mechanism was performed on Li-pretreated AEC. In human AEC, epinephrine (EPI) and methoxamine caused a transient prazosine-and pertussis toxin-sensitive accumulation of IP3 and IP2 and decrease in PIP2. In rabbit AEC, EPI and clonidine caused a transient increase in IP3 and IP2 and decrease in PIP2 and PIP. The time course of changes in IP3, IP2 and PIP2 levels suggests α_2-adrenergic activation of phospholipase C. This finding represents a novel mechanism for α_2-adrenergic receptor in rabbit AEC. Supported by NIH (DK-27651) and National Cystic Fibrosis Foundation.

Tu-Pos113

INITIAL CHARACTERIZATION OF THE INOSITOL-1,4,5-TRISPHOSPHATE RECEPTOR IN A RBL(2H3) CELL MICROSOMAL FRACTION

F.C. Mohr*, I. Zimanyi†, P.E. Chen*, I.N. Pessah† Dept. Vet. Path.* and Dept. Vet. Pharm/Tox†, Univ. of CA, Davis, CA 95616.

Permeabilized rat basophilic leukemia (RBL) cells, release intracellular stored Ca^{2+} in response to inositol-1,4,5-trisphosphate (IP_3). Binding of [^{3}H]IP_3 to its intracellular receptor was studied by equilibrium and kinetic binding experiments on a subcellular fraction from solid RBL tumors. Scatchard plots of binding data indicate a B_{max} of 1.5 pmol [^{3}H]IP_3 bound/mg protein and a K_d of 0.5 to 2 nM. IP_3 binding is affected by pH and [Ca^{2+}] and inhibited by I-2,4,5-P_3, I-1,4-P_2, and heparin. Analysis of data from equilibrium and dissociation experiments reveal the presence of multiple states of the IP_3 receptor. [Ca^{2+}] variations affect the Kd and linearity of Scatchard plots but not the B_{max}. Thus, Ca^{2+} might be involved in the regulation of IP_3 binding. IP_3 appears to release Ca^{2+} from permeabilized cells in a calcium-sensitive manner. The high density of receptor sites from these tumors permits detailed study of IP_3 receptor structure and function. Funded by grants BRSG# 89-13(FCM), NSF Graduate Fellowship (PEC), and NIH#E505002(INP).

Tu-Pos114

CALCIUM TRANSIENTS AND EXOCYTOSIS IN SINGLE NEUTROPHILS

O.Nüsse and M.Lindau Biophysics Group, Free Univ. Berlin, D-1000 Berlin 33,FRG

(Intro. by H. Rüppel)

Membrane capacitance and fura-2 fluorescence were simultaneously measured in human neutrophils using the whole-cell patch-clamp configuration to monitor exocytosis and $[Ca^{2+}]_i$. In the presence of GTPγS in the internal saline $[Ca^{2+}]_i$ starts to increase after ~40s from ~150nM to ~600nM with a sigmoid time course. The peak is reached after ~30s but the main increase occurs within 3s. Within 1-2min $[Ca^{2+}]_i$ subsequently decays to a level close to that before the transient. The Ca transient does not require the presence of extracellular calcium. If IP_3 is included in the internal saline no Ca transient is observed suggesting that GTPγS releases Ca^{2+} from an IP_3 sensitive pool. Exocytosis normally commences at the peak of the transient. However, when the transient is blocked by EGTA exocytosis still occurs but the lag phase is significantly prolonged. These results closely resemble previous observations in mast cells suggesting a similar regulation of exocytosis in both cell types.

Supported by DFG, Sfb 312 / B6.

Tu-Pos115

FURTHER STUDIES ON INTERACTION GEOMETRY DURING RNA SYNTHESIS. P. Chuknyisky, R. Beal, E. Tarien, J. Rifkind, P. Clark and G. Eichhorn. NIH/NIA/GRC, Balto., MD 21224.

We have been studying the interaction geometry of the two initial nucleoside triphosphates (NTP) between which a bond is formed in RNA synthesis. We used EPR to measure the distance between the metals on the two sites to which the NTPs are attached in E. coli RNA polymerase and NMR to measure distances from the metals to the NTPs. These distances change, indicating enzyme flexibility. We hypothesize that this flexibility makes it possible to differentiate between "correct" and "incorrect" NTPs, with only the former being placed into the optimal configuration for bond formation. This hypothesis can be tested by comparing the geometry produced with a variety of substrates and templates. We are presently comparing 3'dATP and poly(dA)·poly(dT) with ATP and poly(dAdT)·poly(dAdT). The former pair allows correct base-pairing but the lack of a 3'OH group in the NTP prevents internucleotide bond formation, while the latter pair contains 3'OH groups on the NTPs but prevents template-NTP base pairing. One of the metals is in position to participate in bond-forming catalysis, while the other presumably is involved in stabilizing the enzyme structure.

Tu-Pos116

THERMODYNAMIC ANALYSIS OF SINGLE SITE MUTANTS OF THE BACTERIOPHAGE LAMBDA cI REPRESSOR THAT ARE DEFECTIVE IN COOPERATIVE BINDING TO DNA

D. Beckett and G.K.Ackers, Department of Biology, The Johns Hopkins University, Baltimore, MD 21218

The cI repressor binds to the right and left operator regions on the bacteriophage lambda genome to control initiation of transcription. Binding of the repressor to adjacent operator sites is cooperative and quantitiative modeling of the action of cI at the two operator regions indicates that cooperativity is crucial for biological function(1). Testing of the model will be greatly facilitated by the availability of single site mutants of the repressor. We have isolated mutants of the repressor that are defective in cooperativity. Intrinsic and cooperative free energies for binding of the repressors to DNA have been determined by quantitative DNAse footprint titration (2). An analytical gel chromatography technique that allows detection of the repressor at extremely low concentrations has been used to directly measure the assembly properties of the mutant repressors. These mutants provide tools for examining the importance of cooperativity to the biological function of cI and for probing the molecular mechanism of cooperative binding of cI to DNA.

1. Ackers, Johnson, and Shea (1982) *Proc. Natl. Acad.Sci.U.S.A.79*,1129-1133. 2. Brenowitz, Senear, Shea, and Ackers (1986) *Meth. in Enzymology 130*, 132-181.

Tu-Pos117

A FLUORESCENCE STUDY OF THE INTERACTION OF PROTEIN SYNTHESIS INITIATION FACTORS 4A AND 4E WITH mRNA AND OLIGONUCLEOTIDE ANALOGS

D.J. Goss[1], S.E. Carberry[1], E. Kapsis[1] & R.E. Rhoads[2]. [1]Hunter College of CUNY, NY; [2]U. of KY, Lexington, KY.

The interaction of eukaryotic protein synthesis initiation factors eIF-4E and eIF-4A with the cap analog m^7GpppG and globin mRNA were probed. The K_{eq} for the formation of binary complexes were obtained from direct fluorescence measurements. An interaction scheme for the formation of a ternary mRNA:eIF-4E:eIF-4A complex was developed, and the coupling free energies, which provide an estimate of the cooperativity of the interaction of eIF-4E, eIF-4A, and mRNA were calculated. These coupling energies were small and positive, indicative of anti-cooperative binding. Further studies of the interaction of eIF-4E with capped oligonucleotides revealed structural features of the mRNA essential for binding.

Grant Support: AHA, NSF86007070 & NIH-GM20818.

Tu-Pos118

SECRETION OF BOVINE SOMATOTROPIN FROM *E. COLI*.

BARBARA KLEIN, STEPHEN HILL, CHRISTINE SMITH, CATHERINE DEVINE, EDWIN ROWOLD AND PETER OLINS. BIOLOGICAL SCIENCES, MONSANTO CO., ST. LOUIS, MO. 63198

One mechanism for the production of a correctly folded protein for reagent protein production or protein engineering studies is the secretion of the protein from *E. coli* followed by osmotic shock to release the proteins from the periplasm. A chimeric protein was constructed in which the lamB secretion signal sequence was fused to the mature coding region for bovine somatotropin. Western blot analysis was used to detect both unprocessed and mature protein expressed from plasmid vectors containing the recA or lacUV5 promoter. The constructs with the recA promoter showed significant protein accumulation without induction; on the other hand the lacUV5 promoter was tightly regulated. Both temperature and inducer concentration had a significant effect on both the total amount of recombinant protein produced and on the fraction processed to mature bST when the lacUV5 promoter was used. The secreted protein was released from the periplasm by a simple osmotic shock procedure and purified using DEAE chromatography followed by reverse phase HPLC. RIA quantitation of the periplasmic fraction showed that 1-2 ug/ml/OD could be released by osmotic shock of benchtop cultures. The secreted protein was also active in the bovine radioreceptor assay.

Tu-Pos119

ACROSOMAL BUNDLE: ACTIN INTERACTIONS
M.F.Schmid[1], P.Matsudaira[2], T.Jeng[3], J.Bordas[4], W.Chiu[1]. [1]Dept. Biochem. Baylor Coll. of Med., Houston,TX 77030, [2]Whitehead Inst., Boston,MA, [3]Abbott Labs, Abbott Pk.,IL, [4]MRC-SERC, Daresbury, UK.

The acrosomal process of the horseshoe crab, Limulus, is a coiled bundle of actin filaments and a binding protein that extends to form a 50μm long straight process called the true discharge. The structure was studied by cryo-electron microscopy because this method produces no staining artifacts, yields higher resolution, and uses near-physiological conditions. Our reconstruction shows that actin filaments are crosslinked by a 102kD protein into a crystalline bundle of filaments. The 102kD protein contacts three actin subunits in an unique intercalative manner. An extension contacts a neighboring 102kD protein. The rigidity of the bundle is likely a consequence of 1) the extensive contacts of actin and 102kD proteins which limit the usual flexibility of the actin filament, and 2) the crosslinks that are formed between filaments in the bundle.

Tu-Pos120

DEHYDRATION OF PROTEIN POLYMERS IN CONCENTRATED NEMATIC SOLUTIONS

Reinhard Hentschke & Judith Herzfeld, Dept. of Chemistry, Brandeis University

Protein fibers [e.g., microtubules and sickle cell hemoglobin (HbS) polymers], formed by the reversible association of quasispherical monomers, contain substantial solvent. Solutions of these fibers become highly non-ideal at high concentrations due to interactions between the elongated particles. One manifestation of this non-ideality is the spontaneous alignment of the fibers. Theoretical calculations based on simple intra- and inter-aggregate interactions leading to polymerization and alignment, agree well with published osmotic pressure data for deoxygenated HbS solutions in the region of the alignment transition. However, at higher concentrations the theory cannot fit the experimental data unless solvent is gradually squeezed out of the fiber under the increasing osmotic stress. We find that a linear potential for fiber dehydration gives osmotic pressure results consistent with the experimental data. Under these conditions, substantial dehydration of HbS fibers occurs with increasing concentrations beyond the alignment transition.

Tu-Pos121

STRUCTURAL STUDIES OF PAP PILI FROM E. COLI

Minfang Gong and Lee Makowski, Department of Physics, Boston University, Boston, MA 02215

Pap pili are filamentous surface appendages of E. coli about 75Å in diameter and 1 μm in length. Expression of these adhesion pili causes E. coli to infect the human urinary tract. Pap pili are composed of a major structural protein and several minor proteins. The major protein, Pap A, is a 15,700 dalton protein composed of 163 amino acids synthesized with a 22-amino acids signal peptide. The bulk of the Pap pili is made up of a helical arrangement of Pap A. We report here the results of X-ray fiber diffraction experiments and scanning transmission electron microscopy of the Pap pili. X-ray diffraction from magnetically oriented fibers was used to determine the helical symmetry of the structure, and the derived mass per unit length was confirmed by scanning transmission electron microscopy. Analysis of scanning transmission electron micrographs of Pap pili suggests an unusual internal structure for the pili. The possible implications of this structure are discussed.

Tu-Pos122

CHROMATOGRAPHY, A MODEL SYSTEM FOR COLLOIDAL FORCES IN THE CYTOSKELETON,

Martin Potschka, Porzellangasse 19/2/9, A-1090 Vienna, Austria.

The cytoskeleton forms a porous network akin to the structure of chromatographic matrices. The permeation of these pores is governed by intrinsic viscosity as shape factor (Anal. Biochem. **162**:47 (1987)) plus a wall effect defined by the energy of interaction between the macromolecular surface and the walls of the pores (J. Chromatogr. **441**:239 (1988)). It may be conveniently studied by varying ionic strength. New data demonstrate a tremendous dependency of the colloidal force of repulsion on the size of the solute polyelectrolyte. The pore size of the cytoskeleton is about 10 Debye lengths in agreement with the separation distance measured for extended molecules. This demonstrates that the stability of the cytoskeleton is based on colloidal forces. If it were not for the observed strong variation with size, small molecules like enzymes, substrates and messengers, could not pass freely through this lattice, and life would not be possible in its present form.

Tu-Pos123

FATTY ACYL CHAIN COMPOSITION, ORDERING AND FLUIDITY IN PLASMA LIPOPROTEINS FROM RABBITS FED FISH OILS.

Regina C. Yang McCabe[1], William Ehringer[2], William Stillwell[2] and Stephen R. Wassall[1] (Introduced by F.W. Kleinhans), Departments of Physics[1] and Biology[2], Indiana University-Purdue University at Indianapolis, Indianapolis, IN 46205.

Rabbits were fed a diet supplemented with either 10% menhaden oil (MO), a fish oil rich in ω-3 polyunsaturated fatty acids (PUFA), or hydrogenated cottonseed oil (HCO) for a period of 12 weeks. Incorporation of ω-3 PUFA's into high (HDL) and low (LDL) density lipoproteins isolated from rabbits on the fish oil diet was monitored by gas chromatography (GC). ESR (electron spin resonance) of 5- and 12-doxyl stearic acids intercalated into the outer amphiphilic monolayer of the lipoproteins did not detect an appreciable difference in order or fluidity between the diets. This contrasts with the inner apolar core where greater fluidity with the MO diet was indicated by fluorescence depolarization of 1,6-diphenyl-1,3,5-hexatriene (DPH) and ESR of cholesteryl 12-doxylstearate.

(Supported by American Heart Association, Indiana Affiliate).

Tu-Pos124

PHASE SHIFTS WITHIN THE AUDITORY HAIR BUNDLE,

R. Keolian, W. Denk and W. W. Webb, Cornell U.

Measurements of the dynamic mechanical impedance of the hair bundle, the motion sensing organelle of the hair cell, show substantial deviations from single pole response--implying that more than one degree of freedom is accessible. Finding that both ends of the bundle move in phase when only the long end is stimulated, we have determined that these extra degrees of freedom cannot be due to the separation of the stereocilia from each other. The unidentified degrees of freedom may arise from an internal viscoelastic relaxation of the elements of the bundle, the active adaptation mechanism that resets the bundle's rest position, or rocking of the underlying cuticular plate in the cytoplasm. The synchrony of motion of the ends of the bundle is consistent with at least three models: 1) all elements of the bundle have the same frequency dependence of their viscoelastic moduli, 2) the stereociliar tips make sliding contact to each other, or 3) the bundle rocks as a single unit. Phase shifts were measured with a differential laser interferometer, while the stereocilia were stimulated with a vibrating glass probe, an oscillating water jet, or with optical tweezers.

Tu-Pos125

CYTOPLASMIC STRUCTURE OF THE BACTERIAL FLAGELLAR MOTOR

Imran H. Khan, Shahid Khan, and Thomas S. Reese*. Depts. of Anatomy and Structural Biology/Physiology and Biophysics, Albert Einstein College of Medicine, Bronx NY 10461. *Lab of Neurobiology, NINDS, NIH, Bethesda MD 20892.

Cytoplasmic basal structures have been visualized in cytoplasm free cell envelopes of the bacterium Salmonella typhimurium by means of rapid freezing and freeze-subsitution. The envelopes were prepared (JBC 256: 8807, 1981) and freeze-substituted (J. Cell Biol. 90: 40, 1981) by standard procedures. The proximal end of the flagellum ends in a characteristic bell shaped structure ~54 nm long and ~48 nm wide surrounding the end of the flagellum. Measuring from the position of the flagellar hook it is likely that the bell extends into the bacterial cytoplasm. The shape and substructure distinguishes it from possible vesicular contaminants adhering to the flagellar base. Stereo analysis of the bell confirms these and other details which suggest that it could be an integral part of the flagellar motor.

Tu-Pos126

UPON MATURATION OF PHAGE T4 CAPSID, ITS MAJOR PROTEIN UNDERGOES A SUBSTANTIAL CHANGE IN SECONDARY STRUCTURE

A Steven[1], H Greenstone[1], A Bauer[1], R Williams[2]
[1] Lab of Physical Biology, NIAMS, NIH, Bethesda, MD 20892;
[2] Biochemistry Dept, USUHS, Bethesda, MD 20814.

We have used laser Raman spectroscopy to investigate the expansion transformation that occurs upon maturation of the T4 prohead. Capsid expansion is accompanied by major changes in its physical and chemical properties, and is preceded in vivo by cleavage of its major protein, gp23 (56K), to gp23* (49K). From their Raman spectra, the secondary structures of precursor (gp23, unexpanded) and mature (gp23*, expanded) polyheads were determined. Similar measurements were also made on uncleaved polyheads expanded in vitro, and on thermally denatured polyheads. We find that the β-sheet contents of both the precursor and mature states of the surface lattice are sufficient to accommodate a domain with the "jelly-roll" fold of antiparallel β-sheets found in the capsid proteins of other viruses. Furthermore, the α-helix content is reduced from 38% to 22% upon expansion, while β-sheets increase from 33% to 45%. We consider two scenarios to account for these data: in one, the changes are largely confined to the gp23-Δ domain - assumed to be initially almost entirely α-helical - that is removed on cleavage of gp23; the other envisages re-folding of gp23* on a much larger scale.

Tu-Pos127

MICROGEL FORMATION AT VERY DILUTE AGAROSE CONCENTRATION.

D. Bulone+ and P.L. San Biagio+*
(+) CNR-IAIF, and (*) Phys. Dept. of University, Via Archirafi 36, I-90123 Palermo, Italy.

QELS data show the existence of freely drifting microgel regions in very dilute, "non-gelling" sols of Agarose quenched from 100 °C to lower temperatures. These structures, whose size depends on concentration and quenching temperature, show a thermal behavior which parallels the gelation of Agarose at higher concentrations. Their existence is not related to the presence of inorganic cores. These results confirm that spinodal demixing plays a central role in the formation of supramolecular structures in this system [1,2,3], and point out that the notion of non-gelling concentration is valid macroscopically only.

1) P.L. San Biagio et al., Biopolymers 25, 2255 (1986).
2) M.B. Palma-Vittorelli, Int. J. Quantum Chem. 35, 113 (1989).
3) P.L. San Biagio et al., Chem Phys. Letters. 154, 477 (1989).

Tu-Pos128

EFFECT OF pH ON THE SIZE DISTRIBUTION OF INTERMEDIATES IN *LIMULUS* COAGULIN POLYMERIZATION. Donovan, M.A. & Laue, T.M. Dept. of Biochem., U. New Hampshire, Durham, NH 03824.
In the final step of coagulation in the horseshoe crab, coagulogen (Mr=21,000) is converted by discrete proteolysis into its clottable form, coagulin. In 0.1 M NH_4HCO_3 50 mM Tris-HCl (pH 8.1), trypsin-generated coagulin rapidly associates to form a stable, solid gel. Polymerization is pH-dependent, with reversible depolymerization occurring in acid (midpoint pH 5.4). Sedimentation velocity analysis reveals that stable intermediates remain at pH 2.5, with 30-31s being the predominant form along with monomer (1.7s) and larger forms (> 60s), see figure. Near the midpoint of the titration (pH 5.4), a pressure-dependent association occurs with a broad distribution of very large species resulting. Supported by NSF BBS 8615815 and the UNH Central University Research Fund.

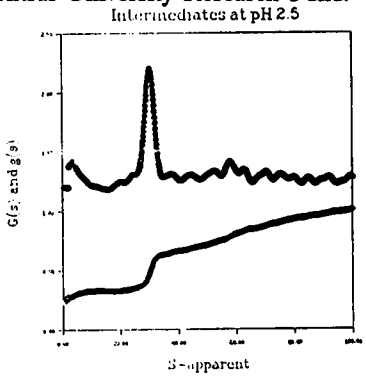

Tu-Pos129

COMPUTER MODELS OF A NEW SICKLE HEMOGLOBIN FIBER. X-Q. Mu & B.M. Fairchild, Columbia University, St. Luke's Hospital Center, 114 St. & Amsterdam Ave. New York, NY 10025

Models have been constructed that are based on an X-ray diffraction pattern of a new sickle cell hemoglobin (HbS) fiber whose layer line spacing is 109Å instead of 64Å as in the "classic" HbS fiber. A search in four-dimensional parameter space showed 12 protofilaments that satisfy the constraints that a) two HbS molecules be related by 2-fold screw symmetry with a translational repeat of 109Å, b) at least one of the substituted residues in HbS, val β6, participate in intermolecular contacts, and c) the energy of intermolecular interaction be <-24kcal/mol.

Seven of each of the 12 protofilament models were close-packed to form a different fiber. Relative protofilament heights in each fiber model were varied to obtain close agreement between the calculated transforms and the observed meridional reflections. Minimization of the fiber packing energy, between -(90 and 130)kcal/mol, and of the R-factor, approximately 21%, yielded 4 fiber models. Determination of a unique model will depend on obtaining higher resolution diffraction data.

Tu-Pos130

CRYO-ELECTRON MICROSCOPY OF DISK AND HELICAL AGGREGATES OF TOBACCO MOSAIC VIRUS COAT PROTEIN. K. Raghavendra*, B. V. V. Prasad+, E. Marietta+, W. Chiu+ and T. M. Schuster*, Dept. Mol. & Cell Biol., Univ. Conn., Storrs CT 06269* and Dept. Biochem., Baylor College of Medicine, Houston, TX 77030+.

Recent studies have indicated that the 20S aggregates of TMV coat protein, which nucleate in-vitro TMV assembly, are helical and 28S aggregates, which crystallize as single crystals of the protein, are dimers of bilayer disks (Raghavendra et al., 1988, Biochemistry, 27, 7583). Both 20S and 28S aggregates undergo extensive association on the grid due to staining and drying artifacts which plague conventional electron microscopy method. In order to confirm our observations that the structure of 20S nucleating aggregates is a helix and not a disk, we have employed cryo-electron microscopy technique which is bereft of these artifacts. Images of 20S, 28S and 17S aggregates (17S is obtained by the dissociation of 28S) embedded in ice have been obtained. These images are being analyzed by using image processing techniques. A comparison of the images of the aggregates obtained by both the electron microscopy techniques will be made. (Supported by NIH grants AI11573 to TMS, RR02250 and GM41064 to WC).

Tu-Pos131

THE EFFECTS OF AMINO TERMINUS DE-ACETYLATION ON THE SUBUNIT STRUCTURE AND SELF-ASSEMBLY PROPERTIES OF TOBACCO MOSAIC VIRUS COAT PROTEIN. K. Raghavendra*, R. Pattanayek+, G. Stubbs+ and T. M. Schuster*, Dept. Mol. & Cell Biol., Univ. Conn., Storrs, CT 06269* and Dept. Mol. Biol., Vanderbilt University, Nashville, TN 37235+.

The coat proteins of tobacco mosaic virus grown in tobacco plants (TMVP) and obtained from recombinant DNA and expressed in E. coli (r-TMVP) have their amino termini acetylated and de-acetylated, respectively (Shire et al. 1987, Biophys. J. 51, 91a). TMVP and r-TMVP exhibit differences in their near-UV circular dichroism spectra and self-assembly properties (Raghavendra et al. 1989 Biophys. J. 55, 156a). The environment of tyrosine 2 appears to be perturbed by the charge on the amino terminus in r-TMVP. A shift towards disk structure has been observed for r-TMVP compared to TMVP under in-vitro virus assembly conditions. We have attempted to explain these differences, by using molecular modeling, based on the known three-dimensional structure of TMVP in the virus (Namba et al. 1989, J. Mol. Biol. 208, 307). Details of possible interactions involving the free amino terminus will be discussed. (Supported by NIH grants AI11573 to TMS and GM33265 to GS).

Tu-Pos132

STRUCTURE OF THE FILAMENTOUS BACTERIOPHAGE PF1 BY X-RAY AND NEUTRON DIFFRACTION - Raman Nambudripad, Wilhelm Stark & Lee Makowski, Dept. of Physics, Boston Univ., Boston, MA 02215.

The filamentous bacteriophage Pf1 is a 2 μm long particle about 65Å in diameter. It consists of single-stranded circular DNA surrounded by 7200 copies of a 46-residue protein which is largely alpha helical. X-ray fiber diffraction pattern from these particles contain data to about 3.3Å resolution. Because of the lack of isomorphous heavy atom derivatives, coordinated use of X-ray and neutron diffraction is being used to characterize the structure of the virus. Neutron diffraction of Pf1 particles with specifically deuterated amino acids has yielded the positions of 15 residues of the coat protein. These have been used to build a model consisting of two almost continuous alpha-helical segments, connected by a non-helical loop stretching from Thr13 to Asp18. This model is now being refined against the X-ray data, which should result in determination of the conformation of the entire coat protein and a detailed description of the protein-protein and protein-DNA interactions in the virions. These will provide a basis for understanding the stability and assembly of the virus particles.

Tu-Pos133

STRUCTURAL STUDIES OF FILAMENTOUS BACTERIOPHAGE M13--Monique Tirion and Lee Makowski, Department of Physics, Boston University, Boston, MA 02215

Bacteriophage M13 is a rod shaped structure approximately 9000 A long and 65 A in diameter, consisting of a circular, single-stranded loop of DNA; five copies each of four end proteins involved in recognition, infection and assembly; and 2700 copies of a 50 amino acid protein subunit, arranged helically around the DNA core. Each subunit of the coat protein is largely alpha helical, with the axes of the alpha helices nearly parallel to the axis of the virus. We are using neutron diffraction from magnetically oriented gels of specifically deuterated virions to characterize the structure of the protein coat. The phage particles are deuterated by growing them in minimal media in the presence of deuterated amino acids. The neutron data, collected at the High Flux Beam Reactor at Brookhaven National Laboratory, extend to 8 A resolution. Initial phasing of the data is done using model building. Difference Fourier maps have been used to determine the three-dimensional positions of the labelled amino acids. Mapping of a substantial proportion of the amino acids on the protein is being used to determine the conformation of the protein on the virus particle.

Tu-Pos134

STRUCTURAL COMPARISON OF FOUR TOBAMOVIRUSES Rekha Pattanayek, Hong Wang, Elizabeth Todderud, Sharon Lobert*, Monicia Elrod and Gerald Stubbs. Department of Molecular Biology, Vanderbilt University, Nashville, TN 37235. *Capstone College of Nursing, University of Alabama, Tuscaloosa, AL 35487

Tobacco mosaic virus (TMV), the U2 strain of TMV, cucumber green mottle mosaic virus (CGMMV-W) and ribgrass mosaic virus (RMV) are all tobamoviruses, with coat protein homologies varying from very close to extremely distant. The structure of TMV has been determined and refined at 2.9Å resolution by fiber diffraction methods. Structural studies are in progress for the others. Similarities in the diffraction patterns clearly demonstrate structural similarities. Calcium binding to carboxyl and phosphate groups is believed to be important in controlling assembly and disassembly of TMV, and the binding sites have been well characterized. Some of the important carboxylates are not, however, conserved in CGMMV-W or RMV. Sequence and structural comparisons suggest that other carboxylate groups in the subunit interfaces could fulfill the same purpose, providing an example of conservation of function in evolution without conservation of primary structure.

Tu-Pos135

A THREE-DIMENSIONAL IMAGE RECONSTRUCTION OF THE ADENOVIRUS TYPE II VIRION BY CRYO-ELECTRON MICROSCOPY

Phoebe L. Stewart[1], Marek Cyrklaff[2], Stephen D. Fuller[2], & Roger M. Burnett[1]
[1]The Wistar Institute, Philadelphia, PA 19104
[2]European Molecular Biology Laboratory, Heidelberg, F.R. Germany

We present a three-dimensional reconstruction of the adenovirus type II virion from frozen-hydrated specimens. The intact virion has a molecular mass of 150×10^6 daltons. The particle is icosahedral with a diameter of 1000 Å and has 300 Å fibers extending from each vertex. Our image reconstruction used the common lines method, which relies on the icosahedral symmetry of the virion to orient projections of numerous virus particles. The resulting three-dimensional density map reveals the distinguishing features of the major capsid protein, hexon, as well as the organization of the 240 hexons and 12 penton bases within the intact capsid. We have confirmed the model for the capsid predicted from the X-ray structure of hexon and images of capsid fragments from conventional and scanning transmission electron microscopy. A new finding is that the thin (40 Å) fibers extending from each vertex are visualized even though they are invisible in the original data. An exciting preliminary finding is that the DNA/protein complex in the core of the virion is organized with icosahedral symmetry.

Tu-Pos136

THE OLIGOMERIC STATE IN SITU OF THE G-PROTEIN SPIKE OF VESICULAR STOMATITIS VIRUS IS A TRIMER

F.P.Booy[1], W.W.Newcomb[2], J.C. Brown[2], A.C.Steven[1] (Intro. by M. Eden)
[1] Lab of Physical Biology, NIAMS, Bethesda, MD 20892; [2] Dept of Microbiology, U.Va. Med. Center, Charlottesville, VA 22908.

Cryo-electron microscopy has been performed on purified VSV particles. In the frozen hydrated state, the three-dimensional shape of the virus is well preserved, and the G-protein spikes are clearly visualized as evenly spaced protrusions around the virion's periphery. In the ice layer, the virus particles are mainly viewed side-on, and have a bullet-like morphology, thus confirming earlier inferences to this effect based on other EM techniques. Spikes are ~9nm long, the inter-spike spacing is ~9.5nm, and the virion is ~170nm in length and ~80nm in width. From these dimensions, we can measure the number of spikes per virion by calculating its total surface area and assuming a quasi-hexagonal close-packing of spikes. On this basis, we find a value of 411, this calculation being somewhat dependent on the radial coordinate used to define the surface (we used the outer surface of the viral membrane), and the overall fraction of surface that is occupied (some bare patches are disclosed in the micrographs). Taking into account our earlier determination of the viral complement of G-protein (1205 $\pm$ 181 copies), we may calculate the stoichiometry of the spike as 2.9 $\pm$ 0.4, i.e. a trimer.

Tu-Pos137

STRATEGY FOR DESIGNING PROTEIN KINASE C INHIBITORS. Remo Bottega and Richard M. Epand, McMaster University, Department of Biochemistry, 1200 Main Street West, Hamilton, Ontario, Canada.

A number of compounds possessing diverse chemical structures are capable of inhibiting protein kinase C. A general property of some of these compounds is that they inhibit bilayer to hexagonal phase interconversion in phosphatidylethanolamine bilayers. In addition, many protein kinase C inhibitors possess a positive charge. We have designed a number of compounds which both incorporate a positive charge as well as bilayer stabilizing ability. In general, these compounds have a hydrophobic backbone which does not perturb the membrane structure and they have a tertiary or quaternary amino group. All inhibit protein kinase C. We also find that the location of the charge may be important. An amphiphile containing an exposed positive charge can inhibit protein kinase C in the 1 to 30 μM range, using the Triton mixed micelle assay. This suggests that a combination of positive charge and bilayer stabilizing ability provides a basis for the rational design of protein kinase C inhibitors.

Tu-Pos138

THERMODYNAMICS OF THE INTERACTION OF INHIBITORS WITH THE BINDING SITE OF RECOMBINANT HUMAN RENIN

D.E. Epps, T.K. Sawyer, M .Prairie, W.C. Krueger, F. Mandel, H. Schostarez, Upjohn Co, Kalamazoo, MI, and J. Cheney, Dept. Chemistry, Harvard University, Boston, MA

The independent subsite (SS) model is widely used for the design of peptide (PEP) Inhibitors (I) of enzymes (NZ) with extended active sites. This model assumes that the SS are independent of each other, and that the free energies of binding contributed by the several SS are additive. We tested the SS model by measuring the thermodynamic binding parameters of a series of PEP I of human renin (HR). Although we found the general mode of binding of these I to be hydrophobic, serious deviations from additivity and SS model constraints were observed. We conclude that an important determinant of binding is probably the conformation assumed by the PEP I in solution. Therefore, that caution be exercised in using affinity constants to assess the interactions of PEP I with HR, and possibly with other NZ having extended binding sites. Furthermore, the thermodynamic parameters for a class of compounds provide more information as to the mode of binding of ligands to their respective receptors than do dissociation constants.

Tu-Pos139

STUDIES ON THE MECHANISM OF ACTION OF ESPERAMICIN.

H. Kishikawa, Y.-P. Jiang, J. Goodisman and J.C. Dabrowiak Department of Chemistry, Center for Science and Technology, 1-014, Syracuse University, Syracuse, NY 13244

The esperamicins and calichemicins are members of an exciting new class of anticancer drug. The natural products possess sugar moieties appended to an unusual bicyclic chromophore referred to as the "warhead". In the presence of reducing agents, the warhead portion of the drug undergoes a rearrangement to a diradical intermediate which is capable of causing a double strand break in DNA. Studies involving a 139-base pair restriction fragment of pBR-322 DNA revealed that the sugars of esperamicin control specificity. Since the cytotoxicity of the drug is believed to be related to its ability to produce double strand breaks in DNA we also studied esperamicin cleavage of covalently closed circular pM2-DNA using agarose gel electrophoresis. Quantitative analysis of the densitometric data showed that the efficiency of double versus single strand breaks is sensitive to the substituents located on the warhead portion of the drug. This work was supported by a grant, NP-681, from the American Cancer Society.

Tu-Pos140

TOPOGRAPHICAL CHARACTERISTICS OF DELTA-OPIOID RECEPTOR SELECTIVE POLYPEPTIDE NEUROTRANSMITTERS

Victor J. Hruby, Om Prakash, Geza Toth, Terry Matsunaga, and Catherine Gehrig Department of Chemistry, University of Arizona, Tucson, Arizona 85721

We have successfully applied the approach of conformational constraints in designing the cyclic enkephalin analogue H-Tyr-D-Pen-Gly-Phe-D-Pen-OH (DPDPE), which has extraordinary δ-opioid selectivity. Utilizing a variety of one and two dimensional NMR methods in conjunction with molecular mechanics and molecular dynamics, we have obtained a low energy conformation model for this molecule in aqueous and DMSO solutions. In order to determine the topographical characteristics and their relationship to receptor selectivity, we have designed over 20 analogues of DPDPE modified at Tyr^1 and Phe^4 residues. The conformations of these analogues have been examined in detail by NMR and other physical methods, and it is observed that large changes in biological activity occur with changes in sidechain topography but not in the secondary structure of the peptide backbone. The results provide a unique insight into the topographical features for μ and δ opioid receptor selective peptides. Supported by U.S.P.H.S. Grant NS19972 & NSF.

Tu-Pos141

POLYACRYLAMIDE AS AN EFFECTIVE DERIVATIZING POLYMER FOR AFFINITY PARTITIONING OF IgG. Donald E. Brooks, D. Skuse and S J. Stocks, Departments of Pathology and Chemistry, University of British Columbia, Vancouver, Canada.

Derivatizing chromatography beads with polyacrylamide can produce immobilization of the non-PEG rich phase in PEG/dextran or PEG/salt liquid two phase mixtures. This observation suggests that polyacrylamide might be an useful agent with which to derivatize molecules to make them incompatible with a PEG-rich phase. We have found this reaction to be a powerful method for directing the partition of proteins in PEG/dextran aqueous two phase systems. We have successfully applied this approach in derivatizing monoclonal antibodies directed against cell surface antigens. They have proven to be the most effective reagents produced to date for the immunoaffinity isolation of cells. Separations of erythrocyte mixtures and transformed lymphocyte lines will be illustrated. Supported by MRC Canada.

Tu-Pos142

Efficient Evaluation of Long Circulating or "Stealth" Liposomes by Studies of *In Vivo* Blood Circulation Kinetics and Final Organ Distribution in Rats.

Martin C. Woodle, Mary S. Newman, Lila R. Collins, and Francis J. Martin
Liposome Technology, Inc., 1050 Hamilton Ct., Menlo Park, CA 94025.

Recent advances in lipid compositions of liposomes have resulted in prolonged blood lifetimes and reduced uptake by the liver and spleen for up to 24 hr. (Allen and Chonn, FEBS Lett, 223, 42, 1987; Gabizon and Papahadjopoulos, PNAS 85, 6949, 1988). To date, demonstration of these capabilities *in vivo* has relied entirely on studies with mice which is limiting in that at least one animal is required for each time point. This method makes kinetic measurements difficult and expensive. Most of the results have been obtained at only one time after intravenous administration of the liposomes. Moreover, while many laboratories have demonstrated similar results with the same formulations, the frequent choice of different timepoints for blood sampling make quantitative comparisons more difficult. Therefore, a technique has been developed with a rat model which provides multiple blood samples from the same animal over the course of 48 hr. with organ distribution at the last time point. Thus, both blood circulation kinetics and a final organ distribution can be obtained from each animal. By using data from the same animal for each time point, greater statisitical confidence can be obtained with fewer animals. Demonstration of several lipid compositions with excellent Stealth properties using the method developed will be presented.

Tu-Pos143

HIGH-EFFICIENCY GENE TRANSFECTION OF ATTACHED MAMMALIAN CELLS BY A RADIO-FREQUENCY ELECTRIC FIELD Q. Zheng and D.C. Chang, Dept. of Mol. Physiol. & Biophys., Baylor Coll. of Med., Houston, TX 77030

Previously, we have reported that by using a pulsed radio-frequency (RF) electric field for electroporation, one can obtain high-efficiency gene transfection in mammalian cells detached by trypsin treatment. Recently, we found that the transfection efficiency could be further improved by avoiding the trypsin treatment. COS-M6 cells growing on coverslips were porated in poration medium (15 mM K-PO_4, 2 mM HEPES, 1 mM $MgCl_2$, 250 mM mannitol, pH 7.3) containing RSV-ß-galactosidase DNA by applying 3 trains of RF pulses (5 pulses per train, pulse width 1 ms, freq. 40 kHz). Expression of ß-gal gene was assayed by histochemical methods at 10 hours after electroporation. At the optimal field strength (0.8 kV/cm), approximately 50% of the cells survived and more than 80% of the surviving cells expressed ß-gal gene. This study thus indicates that a direct application of RF field on attached cells can provide the highest efficiency in introducing genes into cells by electroporation (partially supported by Texas Advanced Tech. Program)

Tu-Pos144

GANGLIOSIDE CONTAINING LIPOSOME-ENCAPSULATED HEMOGLOBIN: FURTHER DEVELOPMENT OF A BLOOD SURROGATE B.A. Goins, K.J. Kestler, V.H. Thourani, A.S. Rudolph and F.S. Ligler, Center for Bio/Molecular Science and Engineering, Code 6090, Naval Research Laboratory, Washington, D.C. 20375

We are currently investigating the utilization of ganglioside G_{M1} as a component in liposome-encapsulated hemoglobin (LEH) to increase LEH circulation persistence. Two incorporation methods were attempted in the preparation of G_{M1}-LEH: 1) co-drying G_{M1} with other lipids and 2) spontaneous incorporation of G_{M1} into preformed LEH. Low rates of G_{M1} incorporation into preformed LEH were noted at 4°C, 23°C and 37°C. Although G_{M1} incorporation was more efficient at 60°C, methemoglobin formation increased dramatically at this temperature, making this protocol undesirable. On the contrary, direct comparison studies of G_{M1}-LEH produced by the co-drying procedure with the current LEH formulation showed that G_{M1} addition did not significantly affect hemoglobin encapsulation efficiency or function. Current efforts to measure circulation half-life and biodistribution of G_{M1}-LEH will be presented.

Tu-Pos145

EFFECT OF FATTY ACID COMPOSITION OF MEMBRANE LIPIDS ON THE ANTIMICROBIAL ACTIVITY OF SYNTHETIC MAGAININS AGAINST *ACHOLEPLASMA LAIDLAWII*.

Douglas Zacherl*, Roy Harris, Elizabeth Macias†, Malcolm Modrzakowski† and Jack Blazyk*, Departments of *Chemistry and †Zoological and Biomedical Sciences and College of Osteopathic Medicine, Ohio University, Athens, OH 45701.

Acholeplasma laidlawii, a mycoplasma possessing no cell wall, is bounded by a plasma membrane similar in many respects to that of a eucaryotic cell. Although this organism is capable of de novo fatty acid biosynthesis, the addition of an exogenous fatty acid to the growth medium results in a substantial enrichment of that fatty acid in the membrane lipids. Thus by altering the length and degree of unsaturation of the fatty acid supplement, the fluidity of the plasma membrane can be modified in a controlled fashion. The lipids extracted from *A. laidlawii* membranes were chromatographically separated and characterized by GC/MS. Lipid phase changes in both whole cells and isolated plasma membranes were detected by FT-IR spectroscopy. The effects of two synthetic antimicrobial peptides, magainin 2 amide and a modified magainin in which two glycine residues were replaced by alanines, on the growth of *A. laidlawii* was measured and correlated to membrane fluidity.

Tu-Pos146

PHOSPHATIDYLINOSITOL BILAYERS STUDIED BY HIGH-PRESSURE INFRARED SPECTROSCOPY,

D. Carrier*, H.H. Mantsch† and P.T.T. Wong†, *Department of Biochemistry, University of Ottawa, Ottawa, K1N 6N5 and †Division of Chemistry, National Research Council, Ottawa, K1A OR6, Canada

The infrared spectrum of aqueous dispersions of soybean phosphatidylinositol has been measured under hydrostatic pressure in the range 1 bar - 20 kbar. The intra- and intermolecular interactions were monitored through the spectral changes observed at increasing pressure in the regions of the phosphate, carbonyl and hydroxyl stretching vibrations. The results indicate the presence of hydrogen bond networks involving the inositol moiety and the phosphate group. The data also suggest a dependence of the conformation of the phosphatidylinositol molecule on the hydration level of its head group. A major structural reorganization of this portion of the molecule was observed at 2 kbar in the nearly anhydrous sample. No similar conformational change could be seen in the hydrated samples, in the pressure range investigated. These influences of hydration and hydrostatic pressure on the conformation of the head group is particularly interesting in view of the role of this lipid as a protein anchor and as a source of second messengers for hormones acting at the cell surface.

Tu-Pos147

FET MEASUREMENT OF INTERPROTEIN DISTANCES IN MEMBRANE PROTEIN AGGREGATES ON SINGLE CELLS.

J.K. Arnette, K.A. Reedquist, B.G. Barisas, and D.A. Roess, Colorado State University, Ft. Collins, CO 80523. Intro. by S. Kinnamon.

A new fluorescence energy transfer (FET) method conceived by T.M. Jovin derives from the reduced rate of irreversible photobleaching of donor (D) fluorophores when acceptor fluorophores (A) are present. Measuring differences in D photobleaching rates on cells labeled with D only (FITC-proteins) and with both D and A (TRITC-proteins) allows calculation of the FET efficiency E. We measured FET on single mouse B-lymphocytes binding various D/A ratios of fluorescent conjugates of tetravalent Con A and bivalent succinyl Con A. For Con A, E attained a maximum value of 0.368 at D/A = 1.67. Assuming a value of 40 Å for r_0, the average inter-lectin distance $\langle r \rangle$ is 43.8 Å. For S Con A, the maximum E was 0.294, corresponding to an $\langle r \rangle$ of 46.3 Å, only 2.5 Å greater than that for Con A. S Con A thus strongly aggregates membrane glycoproteins, rather than behaving as a functionally monovalent lectin. Supported in part by NIH grants AI-21873 and AI-26621 (BGB) and HD-23236 (DAR).

Tu-Pos148

USE OF MONOCLONAL ANTIBODIES (MAb) TO STUDY TOPOGRAPHY OF 3-HYDROXYBUTYRATE DEHYDROGENASE (BDH).

Pascale Adami*, Thomas M. Duncan, J. Oliver McIntyre, Norbert Latruffe*, Clint E. Carter and Sidney Fleischer. Vanderbilt University, Nashville, TN 37235 or *Lab. Biochimie UFR Sciences Univ., Franche-Comte 25030 Besancon Cedex, France.

BDH, a mitochondrial membrane-bound enzyme, has an absolute requirement of phospholipid (PL) for enzymic activity. The beef heart (BH) and rat liver (RL) enzymes are similar by peptide mapping and polyclonal Ab cross-reactivity. Nine anti-BH (five IgG_1 and four IgM) and two antiRLBDH MAb (one IgG_1 and one IGM) have been prepared versus the purified BDH. Only the IgG_1-type MAbs are specific for BDH in mitochondrial membrane by Western blot (WB) analysis. Eight of the MAbs are sequence-specific (SS), positive versus BDH on WB. Two of the SS anti-BHBDH MAbs cross-react with RLBDH and one anti-RLBDH MAb cross-reacts with BHBDH by WB. We are using the MAbs and proteolytic cleavage to map the epitopes of BDH and their orientation with respect to the PL bilayer. Chymotryptic digestion of BDH, reconstituted in PL vesicles, yields a partially active ~25 Kd fragment which remains tightly bound to the membrane [Duncan *et al.*, Biophys. J. 55, 127a (1989)]. Only two of the SS MAbs (one anti-BHBDH and one anti-RLBDH) bind to this fragment. Thus: (i) BHBDH and RLBDH have both common and distinct epitopes; and (ii) at least one common epitope is localized in the ~25 Kd membrane-bound fragment of BHBDH.

[Supported in part by NIH DK 14632.]

Tu-Pos149

A SMALL ANGLE NEUTRON SCATTERING TECHNIQUE FOR THE DETERMINATION OF THE RADIUS OF GYRATION OF INTEGRAL MEMBRANE PROTEINS *IN SITU*.

John F. Hunt, Pierre D. McCrea, Guiseppe Zaccai*, and Donald Engelman. Yale University and (*) Institut Laue-Langevin.

In the past, assessment of the physical size of integral membrane protein complexes has been limited to samples solubilized in non-ionic detergent, a process which may introduce artifacts of unknown scope and severity. A system has been developed which allows the small angle scattering profile of an integral membrane protein to be measured directly while incorporated in small unilammelar phospholipid vesicles. Contrast matching of isotopically substituted phospholipid eliminates the contribution of the bilayer to the observed scattering, resulting in a profile dependent only on the structure of the individual membrane protein complexes and their spatial arrangement in the vesicle. After appropriate correction for their spatial arrangement, information about the molecular weight and radius of gyration of the individual complexes can be obtained. The validity of the technique has been established using monomeric bacteriorhodopsin as a model system.

Tu-Pos150

PRELIMINARY CRYSTALLIZATION STUDIES ON BAND 3, A HUMAN ERYTHROCYTE ANION TRANSPORT PROTEIN.

Manju G. Venugopal and B. A. Wallace, Department of Chemistry and Center for Biophysics, Rensselaer Polytechnic Institute, Troy, New York 12180.

Band 3 is the most abundant protein component in the human erythrocyte membrane. It is a 95,000 dalton glycoprotein which is responsible for exchange of chloride and bicarbonate. Band 3 was purified from fresh human erythrocytes by selective extraction of other protein components. It was then solubilized in N-octyl glucoside and concentrated by ultrafiltration. Microcrystals (dimensions ~0.2 x 0.1 x 0.2 mm) were prepared by the hanging drop vapor diffusion method. Variables explored were detergent/protein ratios, protein concentration, salt type and ionic strength, and precipitant type and concentration. Morphologically distinct forms were prepared from methyl pentanediol (hexagonal) and polyethylene glycol (orthogonal). Preliminary diffraction studies indicate that while the present crystals are somewhat disordered, they diffract to 3 Å resolution. (Supported by NIH DK 39866).

Tu-Pos151

BILAYER STRUCTURE OF A HIGHLY POLYMERIZABLE DIACETYLENIC LIPID

David G. Rhodes[1], Thauming Kuo[2] and David F. O'Brien[2] - [1] Biomolecular Structure Analysis Center, U. of Connecticut Health Center, Farmington, CT 06032 and [2] Department of Chemistry, U. of Arizona, Tucson, AZ 85721

We have used x-ray diffraction to investigate the bilayer structure of a highly polymerizable diacetylenic lipid (JACS 110;7571):

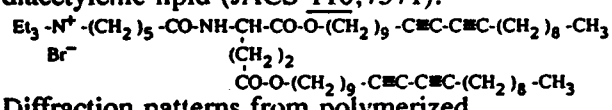

Diffraction patterns from polymerized multilayers of this lipid indicated good lateral ordering, and a considerable degree of mosaic spread. The thickness of hydrated bilayers was ~68 Å. In addition, we observed equatorial reflections corresponding to spacings of 4.4 and 4.8 Å, a ring at ~10 Å, and off-axis reflections. The pattern changed very little upon rinsing the polymerized sample with $CHCl_3$ and remarkable order was still present at elevated temperatures (45°C). We have constructed model structures to fit the lamellar data and have a preliminary model for the in-plane unit cell. We are currently working to refine these structures and to obtain supporting data using other experimental approaches. Supported by NSF (CTS-8904938)[1], the UCHC Research Advisory Council[1], and ACS-PRF-19173-AC7[2]

Tu-Pos152

THE POLYMORPHIC PHASE BEHAVIOR OF ALPHA-TOCOPHEROL HEMISUCCINATE,

Boni,L.T.[1], Perkins,W.R.[1], Minchey,S.R.[1], Bolcsak,L.E.[1], Grumer,S.M.[2], Cullis,P.R.[3], Hope,M.J.[3], and Janoff, A.S.[1] [1]The Liposome Company, Inc., Princeton, NJ 08540, [2]Princeton University, Princeton, NJ 08544, [3]The Canadian Liposome Company, Ltd., North Vancouver, British Columbia, Canada V7M 1A5

The polymorphic phase behavior of α-Tocopherol Hemisuccinate was examined by NBD-PE fluorescence and freeze-fracture electron microscopy. The transition from bilayer to hexagonal II phase can be induced by changes in pH, the addition of Ca^{++}, or the inclusion of tocopherol. Non-bilayer phases were formed below pH 7.5 with hexagonal phase predominating at pH 6.0 and below. The kinetics of the pH induced transition was rapid and increased with increasing temperature and decreasing vesicle size. Lipidic particles formed at 30 mole % tocopherol, with higher tocopherol concentrations forming hexagonal phase. Ca^{++} added at pH 7.5 induced a complex mixture of dehydrated lamellar and hexagonal phases.

Tu-Pos153

FOURIER TRANSFORM INFRARED STUDY OF COLICIN E1 CHANNEL STRUCTURE

P. Rath, O. Bousché, A.R. Merrill†, W.A. Cramer† and K.J. Rothschild.

Dept. of Physics and Cellular Biophysics Program, Boston University, Boston, MA 02215

† Dept. of Biol. Sci., Purdue University, W. Lafayette, IN 47907

Colicin E1 is a 522 residue toxin-like protein whose bactericidal function arises from its channel forming activity. No information is yet available on the structure of the membrane bound form of any colicins. We have studied the structure of the membrane bound state of the COOH-terminal channel forming peptide of colicin E1 (178 residues) by polarised Fourier Transform Infrared Spectrocopy (FTIR). This fragment was reconstituted into DMPC liposomes at varying peptide/lipid ratios ranging from 1/25-1/500. The amide I band of the protein indicated a dominant α-helical secondary structure with limited β-structure. In particular, the amide I and II frequencies are at 1656 and 1545 cm^{-1}, close to the frequencies of the amide I and II bands of bacteriorhodopsin and other α-helical proteins. Polarised FTIR of oriented membranes reveals that the α-helices have an average orientation which is predominantly perpendicular to the plane of the membrane, indicating that the membranes contain α-helices that span the bilayer. (NSF-DMB-8509857, NIH-EY05499-5 (KJR), NIH-GM-18457 (WAC))

Tu-Pos154

MEASURING CHANGES IN BIOMEMBRANE THICKNESS WITH THE SCANNING TUNNELING MICROSCOPE

K. A. Fisher, S. L. Whitfield*, R. E. Thomson*, K. C. Yanagimoto, M. G. L. Gustafsson*, and J. Clarke*. Dept. Biochem. & Biophys. and CVRI, U.C.S.F. 94143, and *Dept. Physics, U.C.B. 94720 and Center for Advanced Materials, L.B.L., Berkeley, Calif. 94720.

We have used scanning tunneling microscopy (STM) to quantify papain-induced changes in the thickness of planar membranes. Monolayers of oriented purple membrane (PM) were prepared on polylysine-treated mica and glass, nitrogen- or freeze-dried, and coated with metal. PM thickness was measured by STM. For STM analysis, programs were designed to select areas of membrane and substrate and to calculate membrane thickness by least squares fitting of two parallel planes. The mean thickness of dried PM was 4.6 nm. Surprisingly, the apparent thickness of enzymatically modified PM increased after papain treatment by 0.2 to 0.8 nm. We conclude that STM of metal-coated planar membrane monolayers can be used to measure changes in average membrane thickness at sub-nanometer resolution. Supported by NIH DA 05043 (K.A.F.) and by DOE DE-AC03-76F00098 (J.C.).

Tu-Pos155

X-RAY DIFFRACTION FROM SYNAPTONEUROSOMAL MEMBRANES FROM RAT CEREBRAL CORTEX

J. Moring, V. Skita, and L.G. Herbette. University of Connecticut Health Center, Farmington, CT 06032

Understanding the interaction of drug molecules with components of the neuronal cell plasma membrane is vital to determining certain drugs' modes of action. At high states of hydration, multilayer samples of synaptoneurosomal membranes yielded x-ray diffraction patterns comprising 5 orders; the d-spacing was ~74A. At lower hydration (84% relative humidity) the pattern changed suddenly to one with a 130A d-spacing and 11 orders. Box refinements indicated that the unit cell was approximately centrosymmetric. Deconvolution of the unit cell Patterson function allowed us to assign phases to the diffraction maxima and calculate an electron density profile. The unit cell (two membranes back to back) probably arises from collapsed membrane vesicles. Either the dihydropyridine Ca^{2+} channel agonist BAY K 8644 or the imidazobenzodiazepine Ro 15-1788 was added to some of the diffraction samples; these drugs appeared to increase electron density primarily in the outer leaflet of the membrane. (Supported by NIAAA center grant #03510, Heublein, Inc., and the Biomolecular Structure Analysis Center).

Tu-Pos156

FREEZE FRACTURING PROPERTIES OF BIOMEMBRANES.

M. Dinda and M.A. Singer, Dept. of Medicine, Queen's Univ., Kingston, Ontario K7L 3N6

When cell suspensions are freeze-fractured, the fracture plane will proceed along the path requiring the least work of separation. For Chinese hamster ovary cells the location of the fracture plane was strongly determined by previous thermal history. Exposure of cells to 40°C for two hours, significantly reduced the probability of a transmembrane fracture plane. This reduction was reversible and decayed within 60 min. In vitro storage of red cells on the other hand, increased the probability of a transmembrane fracture plane. The location of the fracture plane is determined by the relative energy cost of separating apposing monolayers compared to laterally separating lipid in a plane perpendicular to the membrane surface. Our hypothesis is that the relative energy cost is a function of lipid organization.

Tu-Pos157

CHOLESTEROL INTERACTS WITH ALL OF LIPID IN BILAYERS--L. Finegold, Physics, Drexel University, Philadelphia, PA 19104 and M.A. Singer, Medicine, Queen's University, Kingston, Ont. K7L 3N6.

A novel approach to the direct study of cholesterol-lipid interactions in membranes, with complete freedom from added probes, is to measure the effect of added cholesterol (concentration c mol%) upon the main transition enthalpy ΔH of saturated phospholipids of acyl chain length n. Differential scanning calorimetry studies on multilamellar vesicles of phosphatidyl cholines "CnPC", over the largest by far range of n measured, show that $\Delta H = -9.43 + 1.01n - 0.268c$ kcal/mol (for n=12-20), with similar results for the phosphatidyl ethanolamines "CnPE" (for n=10-16). The variation of ΔH with c essentially probes the cholesterol-lipid interaction in the plane of the bilayer, and the variation with n probes deep inside the bilayer. These results give a model in which 12 through 20 carbons of the acyl chains interact equally with cholesterol; the variation with depth is similar for the PC and PE headgroups. The "special concentration" (at which ΔH extrapolates to zero with c) when plotted against n, shows that nine chain carbons are not involved in the transition. This special concentration can provide a physical parameter for other studies (e.g. spin label) in which cholesterol concentration c is varied.

Tu-Pos158

COMPUTER MODELLING OF A MEMBRANE: MEAN FIELD LANGEVIN DYNAMICS OF ONE DIPALMITOYLPHOSPHATIDYLCHOLINE MOLECULE.

H. De Loof, R.W.Pastor, S.C. Harvey, J.P. Segrest. Atheroslerosis Research Unit and Department of Biochemistry, University of Alabama at Birmingham, Birmingham, AL 35294, and Biophysics Laboratory, FDA Bethesda MD 20892.

In order to model the structure and dynamics of phospholipid membranes we extended the single chain Marcelja mean field calculations of Pastor et al. (J. Chem. Phys 89:1112) to one complete phospholipid molecule. The mean field parameters were chosen so as to obtain ageement with deuterium NMR experiments. Both chains behaved very similarly except for the first few carbons of the chain. This asymmetry, due to the kink in the sn2 chain, results in different order parameters for the first methylene groups in the chain. Average dimensions of the molecule were also in agreement with experiment, and pointed toward the cylindrical characteristics of the molecule, necessary for the formation of bilayers. Analysis of the dynamics showed constant dihedral transition rates in the central part of the molecule while increased rates were observed at the end of the chains. The latter effect increased the average local interchain distance and the cone angle describing the wobbling motions of the complete chain. It is also a major factor contributing to the more liquid like behavior in the center of the bilayer.

These results enabled us to start the simulation of a small hexagonally packed model phospholipid monolayer where six mean-field molecules function as the stochastic boundary for a central molecule simulated by standard molecular dynamics.

Tu-Pos159

2-D CRYSTALLINE SHEETS OF CALCIUM ATPASE. Manoj Misra, Kenneth A. Taylor. Dept. of Cell Biology, Duke Univ. Medical Center, Durham, NC 27710

Crystalline 2-D sheets of Ca^{2+}-ATPase can be grown using "standard conditions" described by Pikula *et al.* (J. Biol. Chem., 263, 5277 (1988)). However, such crystals are unsuitable for electron crystallographic studies, because the 2-D sheets aggregate into extended stacks. These stacks can be separated by resuspending pelleted crystals in crystallization medium with 1.0 M sodium propionate substituted for KCl. These attempts at unstacking the 2-D sheets suggested conditions for making large single layered crystalline arrays. Crystalline arrays of up to 3 μm diameter are obtained by incubating deoxycholate purified calcium ATPase (Meissner *et al.*, BBA, 298, 246 (1973)) in standard conditions with Brij 36T detergent at a protein concentration of 0.2-0.5 mg/ml and with 1.0 M sodium propionate. KCl, or $(NH_4)_2SO_4$ at 1.0 M concentration do not have the same effect on stacking or crystal growth that propionate has. The production of 2-D sheets has some dependance on hydrocarbon chain length of the salt because propionate > acetate >> formate. There seems to be no dependance on cation. Membrane stacking depended on propionate concentration. Stacks occur frequently at 0.5 M and no crystals >> 1.0 M. These observations suggests that in addition to reducing the forces that lead to stacking of the sheets, propionate up to 1.0 M concentration may facilitate incorporation of the detergent solubilized protein into the 2-D sheet. Supported by NIH grant GM30598. KAT is an Established Investigator of the American Heart Association.

Tu-Pos160

STRESS *and* STRAIN *in* PATCH CLAMPED MEMBRANES: *Quantitative video microscopy, single channel recording and capacitance.*

F. Sachs and M. Sokabe†. Biophysics, SUNY, Buffalo, N.Y., † Physiology, Nagoya, Japan

Stretch-activated (SA) ion channels respond to membrane tension, but to date there has been no direct measurement of the tension. We have used high resolution DIC microscopy to view patch clamped membranes, and then a non-linear regression algorithm to curve fit images to a geometric model of the patch. This fit provides an accurate estimate of the membrane area and radius of curvature. Knowing the transmembrane pressure we can then calculate the tension. The tension was correlated with changes in area, SA channel activity and patch capacitance.

Conclusions:

1. Membrane lipids flow freely in response to pressure gradients. The lipid capacitance is $0.6 \mu F/cm^2$.
2. SA channel sensitivity is very similar from patch to patch, and only appears different when pressure is used as the independent variable.
3. The elasticity of the membrane is about 20dyn/cm, and represents the elasticity of cytoskeleton, probably spectrin, since pretreatment with cytochalasin-D did not affect the elasticity.

Supported by NIADDK 37792, USARO 26099-LS and the Muscular Dystrophy Assoc.

Tu-Pos161

THE CONFORMATION AND MOLECULAR MOBILITY OF 1,2-DIACYLGLYCEROLS IN PHOSPHOLIPID BILAYERS. James A. Hamilton, Shastri P. Bhamidipati, Dharma Kodali, and Donald M. Small, Biophysics Department, Boston Univ. School of Medicine, Boston, MA 02118

^{13}C NMR spectroscopy was used to study properties of small amounts (1-8 mol%) of 90% ^{13}C carbonyl 1,2 dilauroyl-sn-glycerol (1,2-DLG) in egg phosphatidylcholine (PC) vesicles. A single, narrow carbonyl resonance downfield from two resonances of neat 1,2-DLG was seen. The chemical shift of 1,2-DLG in PC shows that the carbonyl groups are proximal to the aqueous interface, necessitating orientation of the DLG molecule along the normal to the bilayer. Both carbonyl groups are H-bonded to H_2O, but the sn-2 is relatively more hydrated than the sn-1 carbonyl. This conformation of DLG places the glycerol backbone roughly perpendicular to the bilayer plane and resembles that of crystalline and liquid crystalline lamellar PC but not that of crystalline 1,2-DLG. In vesicles the 1,3-isomer of DLG exhibited a narrow carbonyl peak slightly downfield from that of 1,2-DLG. Acyl chain migration from 1,2-DLG to 1,3-DLG was monitored directly in the vesicle by time-dependent NMR measurements.

Tu-Pos162

RECEPTOR REDISTRIBUTION AND CYTOSKELETON-RECEPTOR BINDING AFFECT THE MORPHOLOGY AND STRENGTH OF ATTACHMENT OF CELLS TO LIGAND-COATED SURFACES. Michael D. Ward and Daniel A. Hammer, School of Chemical Engineering, Cornell University, Ithaca, NY 14853.

After initial contact with a ligand-coated substrate, many cells increase their strength of attachment through processes of cell surface and cytoskeletal reorganization (known as "grip-and-stick"). Centrifugal assays show that this increase can be several orders of magnitude.

We report results from mathematical analyses which explain how cell surface and cytoskeletal events modify the morphology and strength of attachment. Using a one dimensional tape-peeling model and a spring model for receptor-ligand bonds, we show how the morphology of the cell-substrate interface depends on receptor number, ligand density, lengths of receptors, ligands and glycocalyx, and membrane mechanical properties when receptors can redistribute. Also, we quantify how receptor and ligand heterogeneity affect the critical applied tension to peel the membrane. Such results show how cells can alter their adhesiveness by regulating receptor composition or secreting ligand. Furthermore, cytoplasmic nucleation centers with binding sites for the cytoplasmic tail of adhesion receptors (eg. cytoplasmic talin molecules) lead to the accumulation of receptors in focal contacts which can increase the strength of attachment many orders of magnitude. The consequences for adhesive behavior of cells with defective cytoskeletal-receptor interactions (eg. tumorigenic cells) will be discussed.

Tu-Pos163

THE EFFECT OF CHIRALITY ON THE BILAYER AND NON-BILAYER PHASE TRANSITIONS IN DI-DODECYL-β-D-GLUCOPYRANOSYL GLYCEROLS.

D.A. Mannock, R.N.A.H. Lewis, R.N. McElhaney, Dept. of Biochemistry, Univ. of Alberta, Edmonton, Alberta T6G 2H7, Canada; D. Turner, S. Gruner, Dept. of Physics, Princeton University, Princeton, N.J., U.S.A., M. Akiyama, Dept. of Physics, Sapporo Medical College, Sapporo, Japan.

Calorimetry and X-ray diffraction have been used to investigate the polymorphic phase behaviour of di-dodecyl-β-D-glucosyl glycerols in which the glycerol is either chiral or racemic. Although the L_β/L_α phase transition temperatures are the same for all three lipids (32.5°C), only the 1,2-*sn*-diastereomer forms a highly ordered gel phase (39.5°C). Furthermore there are significant differences in the bilayer/non-bilayer phase transition temperatures, those of the 2,3-*sn*-diastereomer at 50 and 80°C being 10°C lower than either of the other two compounds. These subtle differences are visible in other short chain glyco-lipids, but disappear at chain lengths longer than 14 carbon atoms, suggesting that the stereochemistry in the headgroup/interfacial regions exerts a stronger influence on the phase behaviour of short chain compounds than it does on long chain compounds, when both are dispersed in water.

Tu-Pos164

THE SUBGEL PHASES OF SATURATED N-ACYL PHOSPHATIDYLCHOLINES: NEW INSIGHTS FROM INFRARED SPECTROSCOPY.

Ruthven N.A.H. Lewis and Ronald N. McElhaney Department of Biochemistry, University of Alberta, Edmonton, Alberta, Canada.

The subgel (L_c) phases of a series of saturated straight-chain diacyl phosphatidylcholines were studied by Fourier-transform infrared spectroscopy. These lipids initially form L_c phases which are similar to that which is formed by incubating aqueous dispersions of DPPC at 0-4°C for 2-4 days. Further storage of most these lipids at low temperatures results in the formation of more stable L_c phases which are spectroscopically distinct from those initially formed. Our data indicate that the formation of these other L_c phases is more favorable with the shorter chain homologues and involve a reorientation of the acyl chains and major hydration changes at the headgroup and polar/apolar interfacial region of the lipid bilayer. We suggest that the process is driven by the formation of a hydrogen bonding network in the headgroup and interfacial region of the lipid bilayer, and that its optimization requires considerable distortion of the optimal packing of the acyl chains. Thus with an increase in acyl chain length the formation of these L_c phases become progressively less favorable and may not be observed with the longer chain homologues.

Tu-Pos165

SOLUBILIZATION AND LOCALIZATION OF WEAKLY POLAR LIPIDS IN UNSONICATED EGG PHOSPHATIDYLCHOLINE: A ^{13}C MAS-NMR STUDY.

Don T. Fujito, Charles F. Hammer, and James A. Hamilton. Chemistry Dept., Georgetown University, Washington, DC, 20057 and Biophysics Dept., Boston University School of Medicine, Boston, MA 02118.

The ability of uncharged, weakly polar lipids to interact with phospholipids and orient at the aqueous interface may be key to their transport and metabolism. We have investigated the interactions of three such lipids - cholesteryl oleate(CO), trioleoyl-sn-glycerol (TOG), and 1,2-dipalmitoyl-sn-glycerol (DPG) - with unsonicated egg yolk phosphatidylcholine (PC) in 50% D_2O by ^{13}C NMR spectroscopy. ^{13}C enrichment of the carbonyl carbon(s) was necessary to monitor the small proportions (0.5-3.0 mol%) of weakly polar lipids. With Magic Angle Spinning (MAS), ^{13}C spectra comparable to those for small unilamellar vesicles (SUV) were obtained. Low levels of TOG (≤2mol%) gave two carbonyl peaks:172.8 ppm (sn-1,3) and 172.3 ppm (sn-2). CO gave a peak at 171.8 ppm which was temperature-independent (30-50°C). DPG showed a single peak at 173.4 ppm from the chemically nonequivalent carbonyl carbons. These chemical shifts were downfield from those of the neat lipids, showing incorporation into the PC bilayer and localization of the polar carbonyl(s) near the aqueous interfaces of the bilayer structure.

Tu-Pos166

TEMPERATURE-JUMP TRC-TEM: A NEW TOOL FOR THE STUDY OF LIPID PHASE TRANSITIONS AND MEMBRANE FUSION

M. Chestnut, J. Burns, D. Siegel[1], and Y. Talmon[2]
[1]Procter & Gamble Co., P.O.B. 398707, Cincinnati, OH 45239-8707.
[2]Dept. of Chem. Eng., Technion-Israel Instit. of Technol., Haifa 32000, Israel.

Time-Resolved Cryo Transmission Electron Microscopy (TRC-TEM) has been used to study intermediates in membrane fusion and L_α/Q_{II} phase transitions [1]. Here we describe a system that rapidly heats TRC-TEM samples immediately before vitrification. Just before the sample is plunged into cryogen, the EM grid is exposed to a focused high-intensity Xenon lamp. As a test, we examined DMPC LUVs. We verified that these LUVs are polyhedral at T < 24°C and round at T ≥ 24°C [2]. We exposed TRC-TEM samples for 0.45 seconds at T = 7 ± 1°C and obtained morphology consistent with a final sample T > 24°C. We also examined films of n-docosane, using electron diffraction to detect the melting (44°C) of initially crystalline films. Xe lamp exposures of 0.15 s induced jumps to T > 44°C from 25°C. Finally, we describe the design and test of a Xe flashlamp system that, in ca. 4 msec, T-jumps samples by 30°C at a time 15 msec before vitrification. [1] Biophys. J. 56, 161 (1989); [2] BBA 812, 493 (1985).

Tu-Pos167

A MODIFIED LEAST SQUARES ANALYTICAL ANALYSIS OF THE HYDRATION, van der WAALS, AND FLUCTUATION FORCES BETWEEN BILAYERS OF DPPC, POPC, AND DOPC. J.M. Collins, Marquette Univ.; B.A. Cunningham, Bucknell Univ.; and L.J. Lis, The Chicago Medical School.

We have used the Rand/Parsegian form of the hydration pressure, the Ninham/Parsegian form of the van der Waals pressure, and the Helfrich model of the fluctuation pressure in order to separate osmotic pressure versus bilayer separation data for DOPC, POPC, and DPPC into estimates of the individual interactive bilayer forces. We used a modified least squares analytic approach (Tamura-Lis, Lis and Collins; JCIS 114, pp214-219, 1986) to estimate the strengths and the decays of these interactive forces. The hydration force decay is sensitive to the model used for the van der Waals force and the fluctuation force. Differences in force parameters for liquid crystalline versus gel state lipids are more significant then for changes in acyl chain composition.

Tu-Pos168

^{2}H NMR ANALYSIS OF LIQUID-CRYSTALLINE GLYCOLIPID DYNAMICS. Beatrice G. Winsborrow, Ian C.P. Smith, and Harold C. Jarrell. Division of Biological Sciences, National Research Council of Canada, Ottawa, Ontario, Canada, K1A 0R6.

Previous work has shown that two types of motion are necessary to describe the partially relaxed lineshapes of the backbone portion of the glycolipid 1,2-di-*O*-tetradecyl-3-*O*-(β-D-glucopyranosyl)-*sn*-glycerol (β-DTGL) in the gel phase. This present study is an extension to the liquid-crystalline phase where more complex motions are anticipated. Powder lineshape and oriented sample relaxation analysis of the backbone region is presented. Application of this approach to the head group, as a test for a unified description of the glycerol (S_{mol} .65) to head group (S_{mol} .45) region, was also attempted. The two gel state motions are a 3 site jump ($\tau_c = 6.7 \times 10^{-10}$s, fast-limit) with site populations .46, .34, .20 and long axis diffusion ($\tau_c = 1.0 \times 10^{-6}$s, slow-limit). In the liquid-crystalline phase the internal jump rate is similar ($\tau_c = 8.9 \times 10^{-10}$s) but the diffusion rate was increased by an order of magnitude ($\tau_c = 8.3 \times 10^{-9}$s, motional minimum) to describe the angle dependent relaxation. The same trend is observed for the head group region; however, at least one other averaging motion is required to account for the head group relaxation profile.

Tu-Pos169

THE EXCHANGE OF DMPC BETWEEN DMPC/DMPE L_α, GEL AND MIXED PHASE LARGE UNILAMELLAR VESICLES

William C. Wimley and Thomas E. Thompson University of Virginia, Department of Biochemistry, Charlottesville Virginia, 22908.

The kinetics of exchange of ^{3}H-DMPC between 70/30 DMPC/DMPE large unilamellar vesicles have been studied by a novel experimental technique. In the liquid crystalline phase (35-55° C) the exchange rates are very similar to those observed in pure DMPC LUV with a similar Arrhenius activation energy of 25.2 kcal/mole. A sharp break in the Arrhenius plot is evident near the temperature at which the vesicles become all gel phase. This is in contrast to the absence of such a break for DMPC exchanging between DMPC/DSPC LUV (*Biophysical J.*(1989),55,114a., *Biochemistry*(1989) in press) thus strengthening our hypothesis that the chain length mismatch of DMPC and DSPC causes packing defects in the gel phase which accelerate exchange over the rates observed in pure DMPC gel phase LUV at the same temperatures. Remarkably, the transbilayer exchange rate of DMPC in the liquid crystalline phase is dramatically reduced (10-100 fold or more) in 70/30 DMPC/DMPE LUV relative to pure DMPC LUV. (Supported by PHS NIH grant GM-14628).

Tu-Pos170

"A REEVALUATION OF THE INTERACTIVE FORCES BETWEEN PHOSPHATIDYLCHOLINE BILAYERS IN MONOVALENT SALT SOLUTIONS"

B.A. Cunningham, Bucknell Univ., J.M. Collins, Marquette Univ., and L.J. Lis, The Chicago Medical School

The iterative technique of B.A. Cunningham and L.J. Lis [J. Colloid Interface Sci. 128, 15 (1989)] is now modified to include a term for the fluctuation force [MacIntosh et al, Biophys. J. 55, 897 (1989)] allowing a reevaluation of the decay constant of the hydration force and the Hamaker constant of the van der Waals force. The addition of a fluctuation force did not cause a change in either parameter for most of the salt solutions studied. The electrostatic force for dipalmitoylphosphatidylcholine bilayers in 1M KBr, however, is found to be nearly constant when the additional fluctuation force is added to the total force analysis as previously predicted by Evans and Parsegian [Proc. Natl. Acad. Sci. USA 83, 7132 (1989)].

Tu-Pos171

A DSC STUDY OF THE EFFECTS OF CHOLESTEROL ON THE MICELLE-VESICLE TRANSITION IN TAUROCHOLATE-PHOSPHOLIPID MIXTURES.

Charles H. Spink & Stephen Manley, Chemistry Department, State University of New York, Cortland, NY 13045.

The thermal transitions of dipalmitoylphosphatidylcholine (DPPC) vesicles contained cholesterol are studied by differential scanning calorimetry (DSC) in the presence of increasing amounts of the bile salt taurocholate (TC). The vesicle, prepared by dialysis, shows marked changes in the thermal transitions in the presence cholesterol as TC is added to levels less than required for solubilization. Other changes occur that reveal how the cholesterol is distributing among the various types of lipid generated as a consequence of the presence of TC. The results are compared with DSC behavior of vesicles without cholesterol. Interpretation of the shifts in T_m, the calorimetric enthalpy and the van't Hoff enthalpy allows conclusions to be drawn about the interactions between cholesterol and phospholipid within the vesicles when solubilization by TC occurs.

Tu-Pos172

COMPOSITION-DEPENDENT CHANGES IN SURFACE STRUCTURE OF CEREBROSIDE-PHOSPHATIDYLCHOLINE MIXTURES.

R.E. Brown, S.B. Johnson, J.M. Smaby, W.H. Anderson, and H.L. Brockman, Hormel Institute, University of Minnesota, Austin, MN 55912

The surface structure of hydrated cerebroside-POPC dispersions has been examined by freeze-fracture electron microscopy. Lipid dispersions were prepared by rehydrating co-lyophilized films comprised of bovine brain cerebroside and POPC at 90°C. After equilibrating at 22°C for 60 min, samples were frozen (liquid Freon). Examination of replicas of the fractured surfaces revealed dramatic changes in surface structure at different cerebroside-POPC compositions. Striking long-range packing order (ripple-structure) was evident between 40 and 80 mole % cerebroside; whereas rippled surfaces were not observed at lower and higher cerebroside compositions. Preliminary cerebroside-POPC monolayer experiments suggest a correlation between composition-dependent changes in surface film behavior (i.e., collapse pressures, predicted molecular areas at different surface pressures) and observed surface structure alterations. (Supp. HL08214)

Tu-Pos173

LIPID DYNAMICS IN SMALL VESICLES

L. S. Lepore, J. F. Ellena and D. S. Cafiso, Department of Chemistry, University of Virginia, Charlottesville, VA 22901.

Small unilamellar vesicles, such as those produced by sonication, are convenient and widely utilized as models for lipid bilayers. However, because of the small radii of these vesicles, the lipid packing may be significantly different than in extended lamellar lipid. Several studies have concluded that the molecular order of the lipid is comparable in vesicular and extended lamellar lipid (Finer, *J. Magn. Reson.*, 1974, **13**, 76; Bloom *et al. Biochem.*, 1978, **17**, 5750). Other findings indicate that the lipid order is different in these systems (Korstanje *et al. Biochem. Biophys. Acta*, 1989, **982**, 196.; Palmer *et al. J. Am. Chem. Soc.*, 1984, **106**, 2434, and references therein). To provide further information regarding this difference, we measured the 13C spin-lattice and spin-spin relaxation times of sonicated vesicles, prepared from palmitoyloleoylphosphatidylcholine, and modeled the lipid chain dynamics using a "two-step" model for relaxation in spherical aggregates (Halle and Wennerstrom, *J. Chem. Phys.*, 1981, **75**, 1982). The order parameters that are obtained from this model are smaller than the order parameters typically obtained in extended lamellar systems. These results indicate that the lipid order is substantially less in bilayers with a high curvature than in flat bilayers.

Tu-Pos174

DEVIATION FROM CYLINDRICAL SYMMETRY IN THE INVERTED HEXAGONAL (H_{II}) PHASE IN PHOSPHOLIPID-WATER MEMBRANES.

D.C. Turner and S.M. Gruner, Physics Dept., Princeton University, Princeton, NJ 08544.

Detailed knowledge of the structure of the Inverted Hexagonal (H_{II}) phase in lipid-water systems is crucial toward understanding the lamellar to H_{II} phase transition and the component energies which are involved. We have used x-ray diffraction to solve for the structure, with a resolution sufficient to uncover inhomogeneities in the headgroup and hydrocarbon regions. Both limited and excess water DOPE systems show deviations from cylindrical symmetry of as much as 10%. In particular, variations of shape and density near the headgroup layer tend to increase with decreasing temperature or hydration. Furthermore, an electron density trough occurs in the region where three adjacent H_{II} tubes meet, implying that the terminal methyl groups pack preferentially into the "hole" at that point. Measurement of this anisotropy should lead to a natural way of defining hydrocarbon packing stress. Possible ways of implementing these measurements into the current models of the L_α to H_{II} transition will be discussed. Supported by NIH and DOE and a Garden State Graduate Fellowship to DCT.

Tu-Pos175

PHASE TRANSFORMATIONS OF MEGA-8 STUDIED BY POLARIZING MICROSCOPY, DIFFERENTIAL SCANNING CALORIMETRY AND X-RAY DIFFRACTION.

Stephanie Tristram-Nagle, John F. Nagle and Lavinia M. Wingert. Depts. Biological Sciences and Physics, Carnegie Mellon University and Crystallography Dept., University of Pittsburgh, Pittsburgh, PA.

1-Deoxy -1-(N-methyloctanamido)-D-glucitol (MEGA-8) is one of a series of amphiphiles that possess both lyotropic and thermotropic liquid crystalline properties that are valuable for crystallizing membrane proteins. Polarizing microscopy revealed several crystal morphologies of dry MEGA-8 upon heating to and cooling from the isotropic phase. DSC indicated three major crystalline forms that melt to isotropic (Iso) at different temperatures: solvent crystals→ Iso at 81.0°C (ΔH=33.2 cal/g), needle crystals → Iso at 87.5°C (ΔH=28.3 cal/g), and terraced crystals →Iso at 78.4°C (ΔH=28.2 cal/g). From the DSC data a Gibbs free energy diagram was constructed identifying the needle crystals and the isotropic phase as the lowest free energy forms over the temperature range 20° C to 100°C. Powder X-ray diffraction confirmed three major crystalline forms. The possibility of a liquid crystalline form will be discussed.

Tu-Pos176

METHOD FOR SELF-ASSEMBLING BILAYER LIPID MEMBRANES ON SOLID SUPPORT

H. Ti Tien and Zdzislaw Salamon, Physiology Dept., Michigan State University, East Lansing, MI 48824

Single bilayer lipid membranes (BLM) separating two aqueous solutions were reported a quarter century ago (1). Mechanical stability has been a common concern, as BLMs rarely last more than a few hours. For long-term studies and for practical applications, as in biosensors and molecular devices, a long-lasting BLM is highly desirable. We report a novel method for forming stable self-assembled BLM on solid support (2). Our simple method is based on interactions between a nascent metallic surface and amphiphilic lipid molecules. One outstanding advantage of this technique is that mechanical stability is greatly improved, by orders of magnitude. In view of their molecular dimensions, dynamic properties, and similarity to biomembranes, such self-organized lipid bilayers are noteworthy.

(Supported by NIH Grant GM-14971-23.)

(1) I.B. Ivanov, ed., "Thin Lipid Films: Fundamentals and Applications," Marcel Dekker, Inc., N.Y., 1988, pp.927-1057.
(2) H.T. Tien and Z. Salamon, Bioelectrochem. Bioenerg., (1989) in press.

Tu-Pos177

MEMBRANE PROTEINS SENSITIZE SONICATED LIPID VESICLES TO RADIATION DAMAGE.

Todd Silverstein, Chem. Dept. Willamette Univ., Salem, OR 97301 and Lester Braby, Radiological Biophysics, Battelle Pacific NW Lab, Richland, WA 99352.

We have previously (Biophys. J.(1989) 55, 115a) measured the Ca++ leakage rates of sonicated phosphatidyl choline (PC) vesicles irradiated with up to 1MRad (from a van de Graaf generator). We found that large radiation doses caused only a slight, statistically insignificant increase in Ca++ leakage relative to non-irradiated control vesicles. This is presumably due to the extreme mechanical stability of these small (250-300 Å diam.) spherical bilayer vesicles, perhaps explaining their resistance to attack by hydroxyl radicals.

In a series of experiments we reconstituted membrane proteins (glycophorin A and low density lipoprotein) into sonicated PC vesicles. We found a significant radiation-induced Ca++ release, from 10-25% release in controls to 40-50% release in irradiated vesicles. Furthermore, this release showed a linear dose dependence from .25 to 1MRad. Future experiments will measure the extent of lipid peroxidation in the membranes in an attempt to specify the mechanism of protein-enhanced radiation damage to lipid membranes.

Tu-Pos178

APPLICATION OF NICOMP 370 SUBMICRON PARTICLE SIZER TO DPPC VESICLE FUSION SYSTEM.

Stephen E. Schullery and Robert C. Piotrowski, Chemistry Department, Eastern Michigan University, Ypsilanti, MI 48197.

Attempted use of the Nicomp 370 dynamic light scattering instrument to study gel-state fusion of DPPC vesicles is reported. Both DPPC SUV and fused vesicles are much more tightly aggregated than previously believed, and not easily disaggregated by heating, stirring or incorporation of antifusogens. Some disaggregation of unstirred heated samples could be effected by mixing with millimolar sodium dodecylsulfate, or the supernatant of Sepharose CL-2B.

The instrument can resolve up to trimodal distributions, assuming either solid or thin-walled "vesicle" particles, and weighting by scattered light intensity, particle number, or volume. An unknown portion of sample can be contained in very large aggregates, which the instrument labels "residual" and attempts with limited success to ignore. Distribution results are then very sensitive to range parameters input by the user. Proper mass weighting for a SUV/fused vesicle mixture is roughly midway between the instrument's values for solid particles and vesicles (thin-walled).

Tu-Pos179

EFFECT OF α-TOCOPHEROL ON PHOSPHOLIPID BILAYER STABILITY. William Stillwell[1], William Ehringer[1], Lijuan Wang[2], and Stephen R. Wassall[2]. Department of Biology[1] and Physics[2], Indiana University-Purdue University at Indianapolis, Indianapolis, IN 46205.

It has been proposed that in membranes α-tocopherol supports two major roles, that of an antioxidant and as a structural component of membranes. Here we report the effect of α-tocopherol on a series of phosphatidylcholine (PC) bilayers composed of either saturated or unsaturated acyl chains. By monitoring carboxyfluorescein leakage from the PC vesicles α-tocopherol is shown to alter membrane permeability. Employing a series of DOXYL stearic acid spin probes, the vitamin is shown to increase order higher in the acyl chains (positions 5 and 7) and decrease fluidity lower in the chains (positions 12 and 16). The effect is greater with a saturated chain (dimyristoyl-) PC than with unsaturated (dioleoyl-, dilinoleoyl-, dilinolenoyl- and diarachadonyl-) PC. The results are generally confirmed by fluorescence polarization of a series of anthroyloxy stearic acid fluorescence probes (positions 2, 6, 9, and 12 on the acyl chains). With the exception that by fluorescence a larger effect of α-tocopherol on decreasing fluidity is noted with the unsaturated PC's than was measured by ESR. α-Tocopherol decreases bilayer membrane fluidity.

Tu-Pos180

PHASE TOPOLOGY FOR SHORT-CHAIN LECITHIN / LONG-CHAIN PHOSPHOLIPID UNILAMELLAR VESICLES Jinru Bian & Mary F. Roberts, Deparment of Chemistry, Boston College, Chestnut Hill, MA 02167

Small unilamellar vesicles form spontaneously from gel state long-chain phospholipids such as dipalmitoyl-PC (DPPC) and short-chain lecithins (e.g., diC_7PC) which by themselves form micelles. When the particles are incubated at temperatures greater than the T_m of the long-chain PC, the particles rapidly fuse (from 90Å to $\geq$ 5000Å radius); this transition is reversible. A possible explanation for this behavior involves patching or phase separation of the short-chain component within the gel-state vesicle and randomization of both lipid species above T_m. ^1H T_1 values of proteo diC_7PC in d_{62}-DPPC/DPPC matrices of varying deuterium content, solid-state ^2H NMR spectrsocopy as a function of temperature, and fluorescence pyrene excimer-to-monomer ratios as a function of diC7PC/DPPC provide evidence that such phase separation must occur. From these results a detailed geometric model for the particles is proposed.

Tu-Pos181

LOCALIZATION OF GLYCOSPHINGOLIPIDS IN PHOSPHATIDYLCHOLINE LIPOSOMES CONTAINING LATERALLY SEPARATED GEL AND FLUID PHASES. *P. Rock, M. Allietta, W.W. Young, T.W. Tillack and T.E. Thompson (sponsored by Ronald P. Taylor). Departments of Biochemistry and Pathology, University of Virginia, Charlottesville, Virginia 22908.*

Multilamellar liposomes composed of 1:1 dielaidoyl phosphatidylcholine : dipalmitoyl phosphatidylcholine, at 20°C, contain laterally separated gel and liquid crystalline phases that can be distinguished by electron microscopy in freeze etch replicas. Visualization of marker proteins which specifically bind to glycosphingolipids included in these liposomes has revealed that at 1 mol % or less, the ganglioside GM_1 and the neutral species asialo-GM_1 are localized within the gel-phase regions. Increasing the mole fraction of the glycolipids results in the appearance of marker in the fluid-phase regions. Another neutral glycosphingolipid, Forssman, does not apparently display a phase preference and is found in both phases at a low mol %. The phase localization may be due to the acyl chain composition, which is identical for GM_1 and asialo GM_1 (mainly stearic acid) and heterogeneous for Forssman glycolipid. (Supported by PHS-NIH grants GM-23673 and GM-26234 and NRSA Fellowship GM-12084).

Tu-Pos182

SYNTHETIC CRYOPROTECTANT AND ANTICRYOPROTECTANT GLYCOPHOSPHOLIPIDS AND THEIR INTERACTIONS WITH DIOLEOYLPHOSPHATIDYLETHANOLAMINE (DOPE) BILAYER. Yong-Serk Park and Leaf Huang, Dept. of Biochem., Univ. of Tennessee, Knoxville, TN 37996.

Some sugars, such as trehalose and sucrose, are cryoprotectants against the dehydration damage of the membrane during freeze-thaw. We have covalently linked some sugars to the amino group of DOPE and examined the cryoprotectant effect of these synthetic glycophospholipids. Liposomes composed of 75% sugar-DOPE and 25% DOPE were subjected to 5 cycles of freeze-thaw and the leakage of entrapped calcein was measured. Isomaltotriosyl DOPE (IMT-DOPE) and neuraminolactosyl DOPE (NANL-DOPE) showed good cryoprotectant effect; whereas lactosyl DOPE (Lac-DOPE) and galactosyl DOPE (Gal-DOPE) had no effect. Furthermore, liposomes containing Lac-DOPE and Gal-DOPE could not be protected by trehalose against freeze-thaw damage. Therefore, Lac-DOPE and Gal-DOPE are anticryoprotectants. FTIR studies showed that trehalose could H-bond with dry NANL-DOPE, but not with dry Gal-DOPE. These results indicate that the anticryoprotectant effect of some glycophospholipids is due to their inability to interact with trehalose at the dehydrated state of the membrane during freeze-thaw. Supported by NIH grants CA24553 and AI25834.

Tu-Pos183

PHASE FLUCTUATION IN PHOSPHOLIPIDS REVEALED BY LAURDAN FLUORESCENCE

T. Parasassi[1], G. De Stasio[2], A. d'Ubaldo[1], R. Rusch[3] & E. Gratton[3]. [1]*Ist. Med. Sper., CNR, V.Marx 15, 00137 Rome;* [2]*Ist. Strut. Mat., CNR, V.E.Fermi, 00044 Frascati, Rome;* [3]*UIUC, LFD, 1110 W. Green St., Urbana, IL 61801.*

The properties of membrane proteins can be influenced by the organization of the surrounding lipids. We used Laurdan to study phase coexistence and interconversion in membrane model systems. Fluorescence properties of Laurdan provide a unique possibility to study lipid domains because of the different excitation and emission spectra of this probe in gel and liquid-crystalline phase. The difference in excitation spectra allows photoselection of Laurdan molecules in one of the two phases. Using the difference in emission spectra, we observed interconversion between the two phases. Experiments were performed in DPPC vesicles at various temperatures, particularly in the region of the phase transition, where phase coexistence and interconversion between phases is likely to be maximal. We also performed time-resolved experiments to directly prove the interconversion process. We found that in DLPC-DPPC mixtures, at 20°C, phase interconversion occurs in about 30-50 ns.
(Supported by PHS-1-P41-RR03155 & CNR.)

Tu-Pos184

MOLECULAR MODELING OF LIPID SYSTEMS FOR COMPARISON WITH EXPERIMENTAL X-RAY DIFFRACTION DATA. Steven L. Blechner[1,2], David G. Rhodes[1] and Victor Skita[1], [1] Biomolecular Structure Analysis Center, UConn Health Center and [2] UConn Department of Physics. Model molecular structures of various lipid systems have been compared to the experimental results of X-ray diffraction experiments using an electron density reconstruction method. Model lipid structures produced with the CHEM-X molecular modeling software were evaluated for feasibility by the following method based on the assumption that the model molecule was packed in a crystalline array. Using the atomic coordinates of the model structure, the number of electrons associated with each atom were added in a region of x corresponding to the Van der Waals radii. Assuming that all lipids are in identical conformation and uniformly packed, this function is proportional to the electron density profile along the bilayer normal. These model profiles were Fourier transformed to produce the continuous one dimensional structure factor ($F(\sin\theta/\lambda)$). This function was sampled at intervals of 1/d, with phases assigned according to the sign of ($F(\sin\theta/\lambda)$). The model structure factors were calculated at the same resolution as the experiments. The resulting F(h/d) could be squared for direct comparison to the raw intensity data or Fourier transformed again to yield a calculated electron density profile for comparison to the experimentally determined profile. Similar reconstructions were used to create non-lamellar intensities from model structures for comparison with off-axis data. Supported by: NSF-CTS-8904398, and UCHC Research Advisory Council.

Tu-Pos185

MOLECULAR MODELING OF LIPID AND LIPID/AMPHIPHILE COMPLEXES
Eric M. Billings, Leo G. Herbette and David G. Rhodes Biomolecular Structure Analysis Center, U. of Connecticut Health Center, Farmington, CT 06032

Molecular models of lipid micelles and bilayers were constructed to examine the structural behavior of lipid complexes. AMBER was used to compute minimum energy configurations and dynamic trajectories for phospholipid micelles with and without amphiphilic ligands. The preferred conformations of the lipids were evaluated in terms of radial distribution functions of torsion angles and atom positions; and the composition of the total energy (steric, electrostatic, etc.). The ligand energetics were examined with regard to time averaged radial position, conformation, and interactions with the lipid environment. The average conformation of a ligand in this asymmetric environment is generally dissimilar to the experimentally determined structure of the molecule in a crystal, or of the computed minimum energy structure in a homogeneous environment. We are currently extending this work to similar calculations for a ligand in a lipid bilayer matrix.
Supported by NSF (CTS-8904938), the UCHC Research Advisory Council, AHA, American Health Assistance Foundation.

Tu-Pos186

RAMAN SPECTROSCOPIC AND DIFFERENTIAL SCANNING CALORIMETRIC STUDIES OF THE EFFECT OF ETHANOL ON THE THERMODYNAMIC AND STRUCTURAL PROPERTIES OF DIPALMITOYLPHOSPHATIDYLCHOLINE BILAYERS.
Mark T. Devlin and Ira W. Levin, Laboratory of Chemical Physics, NIDDK, National Institutes of Health, Bethesda, MD 20892.

The effect of ethanol on dipalmitoylphosphatidylcholine (DPPC) bilayers has been extensively studied by X-ray diffraction, fluorescence spectroscopy, NMR and ESR.[1-4] These studies have demonstrated that DPPC bilayers form a novel chain interdigitated gel phase upon the addition of more than 60 mg/ml ethanol. The formation of the interdigitated gel phase causes the onset of (1) thermal hysteresis of the gel to liquid crystalline phase transition and (2) biphasic behavior of the gel to liquid crystalline phase transition temperature. We present here the results of Raman spectroscopic and Differential Scanning Calorimetric studies suggesting that the empirical observations attributed to the formation of the interdigitated gel phase are more properly ascribed to the penetration of ethanol into the DPPC bilayer.

1. Simon, S.A., & McIntosh, T.J. (1984) ***Biochim. Biophys. Acta 773***, 169-172.

2. Nambi, P., Rowe, E.S., & McIntosh, T.J. (1988) ***Biochemistry 27***, 9175-9182.

3. Rowe, E.S., Fernandes, A. & Khalifah, R.G. (1987) ***Biochim. Biophys. Acta 905***, 151-161.

4. Boggs, J.M., Rangaraj, G. & Watts, A. (1989) ***Biochim. Biophys. Acta 981***, 243-253.

Tu-Pos187

FOURIER-TRANSFORM AND DISPERSIVE RAMAN SPECTROSCOPIC STUDIES OF THE PACKING PROPERTIES OF HIGHLY UNSATURATED PHOSPHATIDYLCHOLINES IN MULTILAMELLAR VESICLES

Burton J. Litman[1], E. Neil Lewis[2], and Ira W. Levin[2]
[1]Department of Biochemistry, University of Virginia, Charlottesville, VA 22908, [2]Laboratory of Chemical Physics, NIDDK, National Institutes of Health, Bethesda, MD 20892.

Molecules with varying degrees of unsaturation in their sn2 position are the most common naturally occurring phospholipids. These studies were designed to utilize molecular order parameters derived from Raman spectroscopic measurements to determine the structural consequences of introducing increasing levels of unsaturation and concomitant addition of two methylene groups into the sn2 chain. The gel to liquid crystalline phase transition of 1-palmitoyl-2-oleoyl-phosphatidylcholine, 1-palmitoyl-2-arachidonoyl-phosphatidylcholine, and 1-palmitoyl-2-docosahexaenoyl-phosphatidylcholine were all characterized by the changes in intensity ratios in the C-H stretching mode region (I_{2850}/I_{2880}) of their Raman spectra. The derived T_m values were -2, -22, and -2C respectively. Thus, going from an 18:1 to a 20:4 chain in the sn2 position induces a lower T_m, while going from 20:4 to 22:6 actually increases the T_m. Spectra obtained on compounds which model the sn2 acyl chains of the phospholipid molecules studied herein allow an estimation of the temperature dependent behavior of the sn1 acyl chain, independent of the sn2 chain contribution. In addition, analysis of the band shape of the olefinic C=C stretching mode provide information relative to the mobility of the sn2 chain. (Supported by NIH grant EY00548 to BJL).

Tu-Pos188

DSC AND TIME-RESOLVED FLUOROMETRIC INVESTIGATION OF DEHYDROERGOSTEROL IN AN INTERDIGITATED LIPID BILAYER.

Yvonne L. Kao & Parkson L.-G. Chong.
Dept. of Biochem., Meharry Med. Coll., Nashville, TN 37208.

Pure C(18):C(10)PC is known to form highly ordered mixed-interdigitated lipid bilayers below the phase transition temperature. Previous DSC results suggested that cholesterol disrupted the packing of interdigitated C(18):C(10)PC. DSC data of dehydroergosterol (DHE), a fluorescent analog of cholesterol, exhibits similar characteristics to cholesterol in C(18):C(10)PC. Thus DHE is suitable for fluorescent sterol studies. Fluorescent data shows that the rotational motion of DHE can be described by a hindered anisotropic model. The rotational correlation time, θ_2, of DHE decreases montonically in the gel state of C(18):C(10)PC up to 24 mol%, suggesting that DHE causes a disordering/spacing effect on packing of mixed interdigitated C(18):C(10)PC bilayers. θ_2 and DSC values undergo abrupt changes around 27 mol% DHE, suggesting that major reorganization takes place around this concentration. The data echoes the idea that sterols may function in preventing highly ordered lipid formation in interdigitated structures in natural membranes. (NSF)

Tu-Pos189

^{2}H NMR SPECTROSCOPY OF THE LOW TEMPERATURE BEHAVIOR OF BILAYERS CONTAINING DOCOSAHEXAENOYL PHOSPHOLIPIDS.

Judith A. Barry, Theodore P. Trouard, Amir Salmon, and Michael F. Brown. Department of Chemistry, University of Arizona, Tucson, AZ 85721.

A ^{2}H NMR study was performed to compare the low temperature behavior of bilayers of mixed-chain phosphatidylcholines containing docosahexaenoic acid [per-^{2}H-*n*:0)(22:6ω3)PC] to those of the corresponding disaturated PC's [di(per-^{2}H-*n*:0)PC], *n* = 12, 14, 16, 18. The moments of the ^{2}H NMR lineshapes were evaluated in the liquid-crystalline (L_α) and low temperature phases, and the warming and cooling phase transition temperatures were determined. The extent of ordering in the bilayers was compared both within and between the two series of lipids, in order to evaluate the influences of the docosahexaenoyl chain and the saturated acyl chain length. The presence of the docosahexaenoyl chains was found to sharply decrease the phase transition temperatures, cause a substantial hysteresis between the warming and cooling transition temperatures, and remove the linear dependence of the transition temperatures on chain length.

Work sponsored by NIH postdoctoral fellowship EY 06111 (J.A.B.) and NIH grants EY 03754 and GM 41413 (M.F.B.).

Tu-Pos190

^{2}H NMR STUDIES OF PHOSPHOLIPID BILAYERS CONTAINING DOCOSAHEXAENOIC AND ARACHIDONIC ACIDS.

Kannan Rajamoorthi, Theodore P. Trouard, Amir Salmon, and Michael F. Brown (Intr. by N.J. Gibson). Department of Chemistry, University of Arizona, Tucson, AZ 85721.

^{2}H NMR spectroscopy has been applied to comparative studies of phosphatidylcholine bilayers containing ω6 and ω3 polyunsaturated fatty acids, which appear to play different roles in membrane functions. We have synthesized (per-^{2}H-16:0)(20:4)PC and carried out ^{2}H NMR studies of multilamellar dispersions containing 50 wt % H_2O as a function of temperature. The results for (per-^{2}H-16:0)(20:4)PC have been compared to parallel studies of (per-^{2}H-16:0)(22:6)PC. A substantial difference in the phase behavior of the two systems was observed. The orientational order of the 16:0 acyl chain of (per-^{2}H-16:0)(20:4)PC in the L_α phase is less than in (per-^{2}H-16:0)(22:6)PC at the same absolute temperature, and is comparable at the same reduced temperature. However, the spin-lattice relaxation rates R_{1z} of all the segments of the palmitoyl chain of the (per-^{2}H-16:0)(20:4)PC bilayer are higher than those of the (per-^{2}H-16:0)(22:6)PC bilayer at both the same absolute and reduced temperatures. Work sponsored by NIH grants EY03754 and GM41413.

Tu-Pos191

ORDER AND DYNAMICS IN A PHOSPHATIDYLCHOLINE CONTAINING VINYL PERDEUTERATED ARACHIDONIC ACID FROM ^2H NMR. Kannan Rajamoorthi and Michael F. Brown (Intr. by J.A. Rupley). Department of Chemistry, University of Arizona, Tucson, AZ 85721.

To understand the special properties of highly unsaturated phospholipids in membranes, it is essential to study directly the ordering and motion of the polyunsaturated chains. We prepared (16:0)(20:4-d_8)PC, i.e. containing vinyl perdeuterated arachidonic acid (20:4-d_8) at the *sn*-2 position, and carried out ^2H NMR studies as a function of temperature in the L_α phase. De-Pakeing of the narrow powder-type ^2H NMR spectra (θ=0°) showed upon integration three kinds of deuterons: one with a large splitting (30 kHz), two with intermediate splittings (10 kHz), and the remainder with smaller splittings (0.3-5 kHz). The largest and intermediate splittings decreased with increasing temperature; however, the smaller splittings showed a complex trend. Despite the smaller quadrupolar splittings for most of the deuterons, they showed larger relaxation rates compared to the deuterons of the *sn*-1 saturated chain of (per-^2H-16:0)(20:4)PC. No simple correlation seems to exist between the relaxation rates and the quadrupolar splittings of (16:0)(20:4-d_8)PC. Work supported by grants EY03754 and GM41413 from the NIH.

Tu-Pos192

X-RAY DIFFRACTION STUDIES ON THE EFFECT OF ALKANOLS ON DOPE-MEMBRANES UNDER HIGH PRESSURE. P.T.C. So, M.W. Tate, S.M. Gruner and E. Shyamsunder, Physics Dept., Princeton University, Princeton, NJ 08544.

X-ray diffraction studies on DOPE (dioleoylphosphatidylethanolamine) mixed with a sequence of n-alkanols and water have been carried out as a function of temperature and pressure. The studies show that: (i) The bilayer-hexagonal (L_α-H_{II}) phase transition temperature, T_{bh}, is raised by pentanol and the shorter chain alkanols, whereas all longer chain alkanols lower T_{bh}. Pentanol is the most effective alkanol in raising T_{bh}, while hexagonal shows a dramatic reversal: it is the most effective alkanol in lowering T_{bh}. High pressure raises T_{bh} for all alkanols. (ii) All alkanols lower the unit cell spacing, d, in the H_{II} phase. High pressure reverses this decrease. Longer chain alkanols lower d more than shorter chain alkanols. The results will be interpreted in terms of the spontaneous curvature hypothesis of anaesthetic action on lipid layers. This work is supported in part by the ONR (Contract N00014-86-K-0396P00001) and by the NIH (Grant GM32614).

Tu-Pos193

Volatile Anesthetic Effects on Ca^{2+} Uptake by Isolated Canine Cardiac Sarcoplasmic Reticulum

Martha J. Frazer & Carl Lynch III, Dept. of Anesthesiology, Univ. of Virginia Health Sciences Center, Charlottesville, VA

Purified canine cardiac SR was employed to elucidate the contractile depressant mechanisms of volatile anesthetics. A crude microsomal fraction was isolated, phosphate loaded, then separated on a discontinuous sucrose gradient to obtain five fractions (A to E, lightest to heaviest). Ca uptake was measured spectrophotometrically using the Ca-sensitive dye antipyrylazo III; ATPase activity was determined by an enzyme coupled assay. Assays with equivalent anesthetic concentrations were done in sealed cuvettes under anesthetic equilibrated atmosphere. Ruthenium red (RR) was included in some assays to inhibit release via active Ca release channels. RR increased Ca uptake (nmoles Ca/ μg·min) in fraction D (0.162±0.01 vs. 0.244±.003, $p<0.006$), but far less in fraction E (0.123±0.02 vs. 0.137±0.02, $p<0.36$), which appeared to represent more purely logitudinal SR. Coupling ratios (nmole Ca uptake per nmole P_i released) in the absence and presence of RR were as follows (*$p<.05$ vs. control):

Frac.D	Control	2.5% Isoflurane		1.5% Halothane	
no RR	+RR	no RR	+RR	no RR	+RR
0.43±.07	0.64±.07*	0.27±.03*	0.35±.06*	0.18±.02*	0.19±.02*
Frac.E	**Control**	**2.5% Isoflurane**		**1.5% Halothane**	
no RR	+RR	no RR	+RR	no RR	+RR
0.58±.09	0.60±.10	0.55±.13	0.47±.12	0.27±.04*	0.25±.05*

The fraction D coupling ratio in the presence of either halothane or isoflurane was significantly less than control; fraction E, which is uneffected by RR, is significantly depressed only by halothane. Isoflurane may be allowing Ca to leak out of the SR vesicles specifically via the release channel, since the effect is partially reversed by RR. Halothane alters both fractions D and E suggest a more generalized effect on the vesicular membranes.

Tu-Pos194

EPR AND ATPASE MEASUREMENTS ON THE INTERACTION OF MELITTIN WITH SARCOPLASMIC RETICULUM VESICLES.

J. VOSS, J. MAHANEY & D.D. THOMAS. UNIVERSITY OF MINNESOTA MEDICAL SCHOOL, MINNEAPOLIS, MN 55455

We have used nitroxide spin-labels to investigate the physical basis of Ca-ATPase inhibition by melittin in SR. The rotational correlation time of spin-labeled Ca-ATPase measured by ST-EPR is 40-50 microseconds at 25° C. The addition of melittin, a small peptide from bee venom, restricts this rotational mobility, abolishing most sub-microsecond rotational motions at a level of 20 melittin bound per Ca-ATPase. Under similar conditions, the Ca-ATPase activity is inhibited by at least 90%. Spin-labeled lipid probes were used to measure effects on lipid fluidity. At 25° C the binding of 20 melittin per ATPase results in only a 19% and 4% decrease in the lipid fluidity as measured with 5-SASL and 16-SASL probes, respectively. This effect on lipid order is too small to account for the large retardation in Ca-ATPase rotational mobility and is probably too small to account for the enzymatic inhibition. The Ca-ATPase activity is decreased by 50% at 7 melittin bound per ATPase. Therefore, we propose that melittin inhibits the Ca-ATPase by inducing aggregation of the Ca-ATPase in the bilayer. Our conclusion is consistent with previous studies showing a decrease in ATPase activity upon aggregation of the enzyme.

Tu-Pos195

THE EFFECT OF MELITTIN ON MOLECULAR DYNAMICS AND ATPase ACTIVITY OF THE Ca-ATPase IN SARCOPLASMIC RETICULUM.

W. BIRMACHU, J. VOSS, D. M. HUSSEY & D. D. THOMAS. DEPARTMENT OF BIOCHEMISTRY, UNIVERSITY OF MINNESOTA MEDICAL SCHOOL, MINNEAPOLIS, MN 55455.

We have studied the effect of the small basic peptide, melittin, on Ca-ATPase activity and protein and lipid dynamics in skeletal SR using time-resolved and steady state optical spectroscopy. Melittin completely inhibits Ca-ATPase activity with a half maximal inhibition at 7 ± 2 moles of melittin bound per mole of ATPase. The time-resolved phosphorescence anisotropy (TPA) decay of the Ca-ATPase labeled with erythrosin-5-isothiocyanate shows that melittin restricts protein mobility. At 25 °C, in the absence of melittin, the TPA is characterized by three decay components, corresponding to segmental motion, rotation of monomers, and the rotation of oligomers. The effect of melittin is primarily to decrease the amplitude of monomer rotation while increasing the residual anisotropy which corresponds to the formation of large aggregates. Fluorescence anisotropy of the lipid soluble probe DPH shows a maximum of 10 % increase in lipid hydrocarbon chain order, an increase too small to account for the large decrease in protein mobility or inhibition of Ca-ATPase activity. Thus, the inhibitory effect of melittin correlates with its capacity to aggregate the Ca-ATPase, and is consistent with previously reported inhibition of the ATPase under conditions that increase protein-protein interactions.

Tu-Pos196

IMMUNOAFFINITY PURIFIED 106-kDa PROTEIN FROM SARCOPLASMIC RETICULUM (SR) IS A Ca^{2+} RELEASE CHANNEL MODULATED BY AGENTS THAT ALTER Ca^{2+} RELEASE.

by R.J. Hilkert, N.F. Zaidi, C.F. Lagenaur, and G. Salama, The University of Pittsburgh, Dept. of Physiology, Pittsburgh, PA 15261.

In SR vesicles, the oxidation and reduction of a "critical" -SH on an SR protein opens and closes a Ca^{2+} release pathway. The 106-kDa protein involved in sulfhydryl gated Ca^{2+} release was purified by biotin-avidin chromatography, used to immunize rabbits and raise polyclonal antibodies (Abs). Immunoaffinity-purified 106-kDa proteins incorporated in planar bilayers revealed a cationic channel with large unitary conductances for Na^+ and Ca^{2+}. The channel was activated by μM free [Ca^{2+}] and mM [ATP]; inhibited by μM ruthenium red and mM [Mg^{2+}], *ie.*, properties similar to recordings from fusion of SR vesicles and incorporation of "feet" proteins. SH oxidation by 5-20 μM 2,2'dithiodipyridine (2,2'DTDP) resulted in activation of 106-kDA channels such that open probability increased from 0.28 to 0.76. Reduction of disulfides with cysteine or glutathione reversed the 2,2' DTDP effect. Channels activated by Ca^{2+}, ATP, or 2,2'DTDP shifted to a closed state within 45 s after the addition of 5-20 nM ryanodine; in contrast, μM ryanodine is needed to inhibit the conductance of "feet" proteins. Anti-106-kDa polyclonal Abs were effective in modulating channel activity which indicates that the 106-kDa, rather than a contaminating protein, is responsible for the current fluctuations. Thus, the 106-kDa protein is a newly discovered, sulfhydryl gated Ca^{2+} release channel in SR.

Tu-Pos197

OXIDATION OF A "CRITICAL" SULFHYDRYL AND ITS LINKAGE TO BIOTIN IDENTIFIES A 106-kDa Ca^{2+} RELEASE CHANNEL IN SARCOPLASMIC RETICULUM (SR). N.F. Zaidi, C.F. Lagenaur, R.J. Hilkert, J.J. Abramson* and G. Salama, *Portland State University Physics Dept., Portland, OR 97207 and Universtiy of Pittsburgh, Dept. of Physiology, Pittsbugh, PA 15261.

Biotinylated derivatives of reactive disulfide N-succinimidyl 3(2-pridyl-dithio)propionate induce Ca^{2+} release from actively loaded SR vesicles. They oxidize -SH sites on SR proteins via thiol-disulfide exchange and form mixed disulfides between SR protein(s) and biotin. A single 106 kDa SR protein was thus labelled with biotin and purified by biotin-avidin chromatography. Reduction of the disulfide with dithiothreitol closed the Ca^{2+} release pathway causing active reuptake of Ca^{2+} and dissociated biotin from 106-kDa proteins. Incorporation of highly purified 106 kDa protein in planer bilayers revealed cationic channels with large Na^+ (g_{Na^+} = 375 ± 15 pS) and Ca^{2+} ($g_{Ca}2+$ = 107.7 ± 12 pS) conductance, which was activated by μM $[Ca^{2+}]_{free}$, μM Ag^+, mM ATP and blocked by μM ruthenium red or mM $[Mg^{2+}]$. Moreover, the 106-kDa protein is not ATPase, and is not a proteolytic fragment or not a subunit of 400 kDa Ca^{2+} release channel since a) anti-ATPase monoclonal antibody did not cross react with 106 kDa and b) anti-106-kDa polyclonals did not cross react with either ATPase or 400 kDa. Thus the SR contains a sulfhydryl gated 106 kDa Ca^{2+} channel with characteristics similar to the 400 kDa feet protein.

Tu-Pos198

ROSE BENGAL STIMULATES CHANNEL ACTIVITY OF THE ISOLATED 106 kDa Ca^{++} RELEASE PROTEIN FROM SKELETAL MUSCLE SR. Hui Xiong, Edmond Buck, Janice Stuart, *Guy Salama, and Jonathan J. Abramson. Portland State University, P.O.Box 751, Portland OR 97207, and *University of Pittsburgh, Pittsburgh PA 15261.

Low concentrations of the photo-oxidizing xanthene dye rose bengal (10nM to 1μM) stimulates rapid release of Ca^{++} from skeletal muscle SR vesicles. We have recently isolated a protein of molecular weight 106 kDa on the basis of its interaction with reactive disulfide compounds. When it is incorporated into a BLM, it shows Ca^{++} channel activity (~100pS) which is stimulated by ATP, Ca^{++}, and SH reagents. It is also inhibited by Mg^{++} and ruthenium red and is modulated by nanomolar ryanodine. Here we observe that channel activity of the 106 kDa protein is stimulated by 1μM rose bengal without altering channel size. Illumination causes the channel to lock in the open state. The site of action of rose-bengal-stimulated Ca^{++} release appears to be the 106 kDa Ca^{++} release protein from SR. This may be significant because rose bengal appears to mimic photooxidative reperfusion damage in cardiac muscle. Supported by AHA Grant 87 915.

Tu-Pos199

SARCOPLASMIC RETICULUM OF SCALLOP MUSCLE HAS TWO TYPES OF CALCIUM-RELEASE CHANNELS. K. Ondrias, L. Castellani*, B.E. Ehrlich, Depts. Med. & *Physiol., Univ. Conn., Farmington, CT; *Rosenstiel Ctr., Brandeis Univ., Waltham, MA.

Previously we found that sarcoplasmic reticulum (SR) from vertebrate smooth muscle has an IP_3-gated Ca^{2+} channel that is distinct from the Ca^{2+}-release channel found in striated muscle SR. Electron microscopic studies have shown that the SR from scallop striated muscle has morphological features similar to both vertebrate smooth and striated muscle. When SR vesicles from scallop striated muscle were incorporated into planar lipid bilayers, two different Ca^{2+} channels were observed. One channel had a conductance of 80 pS, was activated by caffeine and was inhibited by ruthenium red, as seen with the Ca^{2+}-release channel of vertebrate striated muscle. The other channel was opened by 1 μM IP_3 and was inhibited by heparin, but not by ruthenium red, as found with the IP_3-gated Ca^{2+} channel of vertebrate smooth muscle SR. These results show that scallop SR contains two Ca^{2+}-release pathways and that this invertebrate striated muscle is functionally related to both smooth and striated muscle of vertebrates.

Tu-Pos200

INDUCTION OF CA^{2+} RELEASE FROM SARCOPLASMIC RETICULUM (SR) IS MEDIATED BY CONFORMATIONAL CHANGES OF THE FOOT PROTEIN (FP) T. Ohkusa[a], J.J. Kang[a], V. Heemstra[a], and N. Ikemoto[a,b] (a, Dept. Muscle Res., Boston Biomed. Res. Inst.; b, Dept. Neurol., Harvard Med. Sch.)

SR was labeled with the covalently reacting fluorescent conformational probe, N-[7-(dimethylamino)-4-methyl-3-coumarinyl] maleimide (DACM); major labeling sites were the FP and ~30 kDa protein. Then, the labeled FP was purified. The fluorescence intensity of the FP-attached DACM changed upon the addition of Ca^{2+} release-inducing agents such as polylysine and caffeine. The inducer concentration-dependence of the fluorescence change was identical to that of the induction of Ca^{2+} release from SR, and the fluorescence change preceded the induced release. Furthermore, the $[Ca^{2+}]$-dependence of the fluorescence change was identical to that of the induced release. These results suggest that the trigger-to-release coupling is mediated by the rapid conformational changes of the FP. Preliminary data suggest that the depolarization of the T-tubule also produces similar conformational changes of the FP. (Supported by NIH and MDA)

Tu-Pos201

MAGNESIUM MODULATES INOSITOL (1,4,5)-TRISPHOSPHATE (IP_3) SENSITIVE CALCIUM CHANNELS FROM SARCOPLASMIC RETICULUM (SR).

C. Alcayaga and B.A. Suárez-Isla. (Intr. by: C. Hidalgo). Dept. Fisiol. & Biofísica, Fac. Medicina, U. de Chile and Centro de Estudios Científicos de Santiago, Casilla 16443, Santiago, Chile.

Mg^{2+} is an important modulator of channel gating and is present at 0.8 to 1.6 mM in frog skeletal muscle. We studied its effects on the gating and conduction properties of the IP_3-sensitive Ca^{2+}channel of SR membranes from frog skeletal muscle (Suárez-Isla et al.Biophys.J.,737,54,1988)(POPE:PS:PC=5:3:2 bilayers; 37 mM Ba HEPES trans, 225 mM HEPES Tris cis, pCa 6.0, pH 7.4.) 1) When Mg^{2+} was added to cis (0.1 to 20 mM), shifts of the I/V curves were observed only at $[Mg^{2+}] \geq 2$ mM cis and estimated P_{Ba}/P_{Mg} was 3.2. 2) In contrast, cis Mg^{2+} altered channel gating at 0.1 mM increasing τ_{closed} in a concentration dependent manner. 3) At pCa 6.0, Mg^{2+} (≤1 mM) decreased the $[IP_3]$ needed to increase P_o to 50% of maximum from 5 μM to 0.5 μM. This suggests that under physiological conditions the Ca^{2+} channel from SR could be activated by submicromolar $[IP_3]$.

Supp. by FONDECYT #902, 972 and NIH-GM35981.

Tu-Pos202

ALTERED pH SENSITIVITY OF RYANODINE BINDING TO SARCOPLASMIC RETICULUM OF MALIGNANT HYPERTHERMIA SUSCEPTIBLE (MHS) PIGS.

Rebecca P. Biegon, James R. Mickelson and Charles F. Louis. Veterinary Biology Department, University of Minnesota, St. Paul, MN 55108

The binding of ryanodine (Ry) to pig skeletal sarcoplasmic reticulum (SR) is completely inhibited below pH 6.2 and increases with pH to a maximum (approx. 10 pmol Ry/mg protein) at pH 8.0. The half-maximal increase in binding occurs at a significantly lower pH for SR isolated from MHS pigs compared to normal pigs (pH 6.8 vs. 7.2, respectively). Since Ry binding to the calcium release channel of SR occurs apparently only when this channel is in the open (conducting) state, greater Ry binding reflects a greater open probability of this channel. We conclude that a reduction in muscle cell pH favors channel closure. Furthermore, the altered pH sensitivity of MHS Ry binding would enable the MHS SR channel to remain open during the onset of acidosis. This alteration in the MHS SR channel could explain the elevated calcium release which occurs when the MH response is triggered.

Supported by NIH GM 31382.

Tu-Pos203

CARDIAC SARCOPLASMIC RETICULUM (SR) FROM MALIGNANT HYPERTHERMIA SUSCEPTIBLE (MHS) PIGS DISPLAYS NORMAL [^{3}H] RYANODINE BINDING.

Mark A. Strand, Timothy P. Hanson, James R. Mickelson and Charles F. Louis. University of Minnesota, St. Paul, MN 55108.

Skeletal muscle SR isolated from MHS pigs displays several abnormalities in the ryanodine receptor protein (RyR). That cardiac oxygen consumption rises in an MH episode, and tachycardia and cardiac arrest ensue could indicate that this protein is also abnormal in cardiac muscle. This possibility has been examined by measuring ryanodine binding of isolated cardiac SR vesicles in the presence of 100 mM KCl and 6 μM Ca^{2+}. MHS and normal SR had similar affinities for ryanodine (K_d = 25-26 nM) and receptor content (B_{max} of 11.3-12.4 pmol/mg). Furthermore, MHS and normal SR ryanodine binding was stimulated ($Ca^{2+}_{1/2}$ of 0.46-0.51 μM) and inhibited ($Ca^{2+}_{1/2}$ of 0.71-0.78 mM) by similar Ca^{2+} concentrations. That ryanodine binding to cardiac SR is unaltered in MH indicates that the RyR carries no defect in the heart and that fatal changes occurring in the cardiac muscle in an MH episode are secondary effects.

Tu-Pos204

ISOLATION AND RECONSTITUTION OF THE RYANODINE RECEPTOR (RyR) FROM MALIGNANT HYPERTHERMIA SUSCEPTIBLE (MHS) AND NORMAL PIGS.

James R. Mickelson, Lynn A. Litterer and Charles F. Louis, University of Minnesota, St. Paul, MN 55108

Skeletal muscle SR isolated from MHS pigs demonstrates a greater than normal apparent affinity for ryanodine in the presence of μM Ca^{2+}. To determine if this results from an abnormality in the RyR itself we have purified the RyR of both MHS and normal SR by the CHAPS-solubilization /sucrose gradient technique. In the presence of 100 μM Ca^{2+}, 0.5 M NaCl, 0.25% CHAPS, 0.125% soybean PC, pH 7.0, the purified RyR of both types of pig had B_{max} and K_d values of approximately 350 pmol/mg and 5 nM respectively. However, after reconstitution into egg PC vesicles, and in the presence of 0.1 M KCl, 10 μM Ca^{2+}, pH 7.0, the MHS RyR demonstrated a significantly greater affinity for ryanodine (K_d = 71 ± 4 nM) than the normal RyR (K_d = 146 ± 22 nM); this is similar to the difference in affinity observed in native SR. These results thus support the hypothesis that MH is due to a mutation in the RyR.

Supported by the MDA and NIH GM-31382.

Tu-Pos205

FIBER TYPE AND THE ABNORMAL RYANODINE RECEPTOR IN MALIGNANT HYPERTHERMIA (MH). James M. Ervasti, Timothy P. Hanson, James R. Mickelson and Charles F. Louis
Dept. of Veterinary Biology, University of Minnesota, St. Paul, MN.

The relationship between muscle fiber type and the altered ryanodine receptor in MH susceptible (MHS) muscle was studied in sarcoplasmic reticulum (SR) vesicles isolated from the vastus intermedius muscle of normal (N) and MHS pigs. Analysis of isolated vastus intermedius SR with isozyme-specific Ca-ATPase antibodies indicated that the preparations were predominantly of type I fiber origin. In agreement with our previous results (J.R. Mickelson et al., 1988 J. Biol. Chem. 263,9310-9315) in isolated MHS and N longissimus dorsi (predominantly type II) SR, MHS vastus intermedius SR exhibited a significantly lower K_D for [^{3}H]ryanodine binding than did N SR. The Ca^{2+} sensitivity of [^{3}H]ryanodine binding to MHS vastus intermedius SR was also significantly altered compared to N SR. These results suggest that the altered MHS SR ryanodine receptor is not fiber type specific. Supported by NIH grant GM31382.

Tu-Pos206

HUMAN SR CALCIUM RELEASE CHANNEL: SINGLE CHANNEL PROPERTIES IN NORMAL AND MALIGNANT HYPERTHERMIC SKELETAL MUSCLE. Fill, M., T. Nelson, and E. Stefani. Baylor Col. of Med., Houston TX, and Univ. of Texas Health Sc. Center, Houston TX.

Single sarcoplasmic reticulum (SR) calcium release channels from human skeletal muscle (biopsy) were reconstituted in planar lipid bilayers (5:3:2, POPE:POPS:POPC, 50 mg/ml decane). Contracture response of isolated muscle bundles to caffeine, halothane, and ryanodine were determined as part of the human malignant hyperthermic (MH) diagnostic procedure. Heavy SR microsomes were prepared from muscle not used in contracture tests. Bilayer solutions contained (mM): 350cis & 50trans Cs2SO4, 10 Cs-HEPES (pH 7.4), pCa=5. Release channels from both normal and MH human muscle were pharmacologically identified. Comparison of rabbit and normal human channels reveal that conductance (524 and 510 pS, respectively) and gating properties (open & closed tau) are similar. Caffeine (0.6 mM) changed Po from 0.03 to 0.10 in MH (n=2) and 0.03 to 0.02 in normal (n=2) human channels. Thus, the release channel in rabbit and human are similar, and single SR release channel properties related to the human MH syndrome can be examined using the lipid bilayer technique. Supported by NIH.

Tu-Pos207

TEMPERATURE MODULATION OF THE CARDIAC SARCOPLASMIC RETICULUM CALCIUM-RELEASE CHANNEL. R. Sitsapesan, R.A.P. Montgomery, K.T. MacLeod and A.J. Williams. Department of Cardiac Medicine, National Heart & Lung Institute, Dovehouse Street, London SW3 6LY, U.K.

The effect of cooling on isolated sheep cardiac sarcoplasmic reticulum calcium-release channels was investigated. Channels were incorporated into planar phospholipid bilayers and voltage clamp experiments were performed at 22-24°C and 10-12°C. The free [Ca^{++}] was 80 mM on the luminal side of the bilayer and 10 uM on the cytosolic side. Single channel conductance decreased from 95.8±1.9 pS at 22-24°C to 57.3±3.3 pS at 10-12°C (n=8, $Q_{10} \sim 1.6$). In addition to the decrease in conductance observed with a reduction in temperature, the channel open probability (Po) increased in 71% of channels (n=14). Lifetime analysis indicates that the increase in Po resulting from cooling the calcium-activated calcium-release channel is caused by a reduction in the frequency of closing.

This work was supported by the British Heart Foundation.

Tu-Pos208

CARDIAC SARCOPLASMIC RETICULUM:RAT VS. DOG. G.E. Taffet & C.A. Tate, Baylor Col. Med., Houston, TX 77030

Unlike dog heart SR, rat heart SR has a high Mg-dep. (basal) ATPase activity attributed to contamination. Rat SR at 36% sucrose has high basal ATPase like the crude SR with minimal SL markers. Though antibodies to ectoATPase and SR CaATPase cross-react with only the 100K-Da region on 1-D SDS-PAGE, 2-D SDS-PAGE shows only one protein (pI 5) in the 100k-Da region with identical mobility as dog CaATPase. Unlike dog SR, rat SR is sensitive to DTT. With DTT during isolation, basal ATPase of rat SR is low at 50 uM ATP. At 50 uM ATP Ca-dep. ATPase activity is similar between species with a Km for Ca of 5 uM, the same Ca-dep. EP content, and nH = 2. Ionomycin doubles CaATPase activity in both. In rat (not dog) a stimulation of basal ATPase occurs at ATP > 100 uM. Thus, the basal ATPase of rat heart SR is part of the enzyme cycle of the CaATPase, not contamination.

Supported by NIH (AG06221, AG00428, and HL13870).

Tu-Pos209

CALCIUM RELEASE BLOCKERS AND NUCLEOTIDE SPECIFICITY OF CARDIAC SR. G. Shin, C. Tate, & M. Entman. Baylor Col. Med., Houston, TX 77030

In dog cardiac SR, like ATP GTP induces Ca accumulation which is released by A23187. Unlike ATP hydrolysis, however, GTP hydrolysis is not Ca-sensitive or A23187 stimulated. Numerous data support the notion that both nucleotides are hydrolyzed by the CaATPase. Here we explored this paradigm using Ca release blockers. With ryanodine, ruthenium red, or high Mg, ATP-induced Ca accumulation was increased with ryanodine>ruthenium-red>Mg. CaATPase activity was inhibited under these conditions and was relieved by A23187. Like ATP-induced Ca accumulation, GTP-induced Ca accumulation was increased with these blockers with the same order of potency. In contrast to the CaATPase activity, however, GTPase activity was not altered by these agents or by A23187. These data suggest that these agents may also stabilize a nontranslocated pool of calcium not involved in feedback inhibition of nucleotide hydrolysis.

Supported by NIH (HL13870 and AG06221).

Tu-Pos211

CHARACTERIZATION OF cDNA CLONES FOR CHICKEN CARDIAC PHOSPHOLAMBAN.

T. Toyofuku, A. Stewart* and R. Zak.
Departments of Anatomy*, and Medicine, University of Chicago, Chicago, IL 60637.

Intro. by B. Block.

Phospholamban is a 53 amino acid SR membrane associated protein thought to modulate the activity of the Ca-ATPase. To study its structure-function relationship in a non-mammalian system, oligonucleotide probes complementary to the coding region of the dog cardiac phospholamban were used to screen a chicken heart cDNA library. Two overlapping clones were isolated. Sequence analysis revealed a 364bp 5' nontranslated region and the 159bp coding region followed by a long 3' untranslated region which does not contain the AATAAA polyadenylation consensus sequence. The coding region shares 83% homology with the dog phospholamban at the amino acid level. Northern blot analysis shows that cardiac phospholamban is expressed in the chicken heart and slow tonic anterior latissimus dorsi muscle and to a lesser degree in the fast twitch pectoralis and posterior latissimus dorsi muscles. Two predominant mRNAs, 0.8kb and 1.2kb, as well as 2 minor bands at 4kb and 8kb were seen.

Tu-Pos210

INTERACTIONS OF CALCIUM AND LANTHANIDES WITH THE SARCOPLASMIC RETICULUM ATPase. D. Bigelow, T. Squier, F. Fernandez-Belda, and G. Inesi. Univ. of Maryland at Baltimore.

We find that : (a) lanthanides (Ln^{+3}) bind in excess of the specific Ca^{2+} site stoichiometry, mostly to membrane lipids and non-ATPase proteins; (b) however, Ln^{+3} concentrations as low as 10^{-7} M displace Ca^{2+} from the specific ATPase sites, with diphasic kinetics attributable to sequential exchange; (c) while Ca^{2+} activates the entire ATPase cycle, Ln^{+3} allows formation of a phosphorylated enzyme intermediate that undergoes slow hydrolytic cleavage; (d) while Ca^{2+} affects the quantum yield of tryptophan residues (transmembrane region) as well as of the FITC label (extramembranous region), Ln^{+3} induces only a change in the quantum yield of the FITC label; (e) these measurements, as well as energy transfer between bound Ln^{+3} and fluorescent labels, suggest that the Ln^{+3} involved in these effects do not reside in the intramembranous domain identified by mutation experiments (Clarke et al., Nature 339, 476, 1989), but in the stalk region of the ATPase. Both the stalk and transmembrane regions may provide acidic residues for sequential binding of two cations, in which Ca^{2+} binding to the transmembrane region normally allows the cooperative binding of one additional Ca^{2+} to the stalk.

Tu-Pos212

IMPORT OF THE IRON-SULFUR PROTEIN OF THE BC_1 COMPLEX INTO YEAST MITOCHONDRIA. W.W. Fu, S. Japa, and D.S. Beattie, Dept. Biochem. WVU, Morgantown, WV 26506

The gene for the Rieske iron-sulfur protein of the b-c_1 complex was subcloned into the expression vector, SP6-4, transcribed and translated in a reticulocyte lysate in the presence of [^{35}S]-methionine. The time course in vitro of import of this protein into isolated yeast mitochondria at 18° revealed the sequential processing of a precursor (p) form to an intermediate (i) form and mature (m) form. Both i and m forms were resistant to exogenous proteinase K. Mitoplasts (lacking the outer mitochondrial membrane) could also process the p form to both i and m forms suggesting that both proteases are localized in the inner membrane-matrix fraction; however, the m form was then proteinase K-sensitive. Extraction with digitonin indicated that the i form is present in the matrix and the m form on the external surface of the inner membrane. At temperatures below 12°, the i form accumulated in the matrix and could be chased to the m form at higher temperatures. Various concentrations of EDTA and o-phenanthroline could block either processing of the p to i or the i to m form suggesting that both proteases require metal ions. Supported by NSF DCB-8716338

Tu-Pos213

SIGNAL PEPTIDE NET HYDROPHOBICITY DICTATES FUNCTION. M.M. Chou, S.K. Doud and D.A. Kendall Laboratory of Bioorganic Chemistry and Biochemistry, Rockefeller University, New York, NY 10021 and Dept. Molecular and Cell Biology, University of Connecticut, Storrs, CT 06269.

Using homopolymeric units of either isoleucine, leucine, valine or alanine to replace the natural core segment of the E. coli alkaline phosphatase signal peptide, the hydrophobicity requirements for export and processing were delineated. The transport properties of these mutants demonstrated that the net hydrophobicity determines the total extent of precursor processing, while a high mean hydrophobicity per residue is critical for complete, rapid processing and translocation. The preceding conclusions were supported by "titration" of a signal peptide containing a core of low hydrophobicity (10 alanines) with residues of greater hydrophobicity (leucine), thus restoring function. Moreover, alkaline phosphatase was converted from a periplasmic to a membrane-anchored protein via a signal containing 20 leucine residues. This application of polymeric sequences allows systematic comparisons to be made, unambiguously revealing the hydrophobicity requirements governing specific steps in the transport process.

Tu-Pos214

FURTHER STUDIES ON MITOCHONDRIAL CoA TRANSPORT: EVIDENCE FOR NET UPTAKE AND EFFLUX OF CoA. Arun G. Tahiliani and Bhageshri A. Tahiliani, Weis Center for Research, Danville, PA 17821.

CoA uptake into isolated rat heart mitochondria, studied by determining [^{14}C]-CoA associated with mitochondria or by enzymatically determining the mitochondrial CoA content following incubation with CoA was identical. A large proportion of [^{14}C]-CoA associated with mitochondria was readily converted to acyl [^{14}C]-CoA in the presence of various substrates. Addition of exogenous CoA, valinomycin or nigericin to mitochondria preloaded with [^{14}]C-CoA caused a slow dissociation of radioactivity from mitochondria which could not be accounted for by displacement of bound CoA. While the effect of nigericin was comparable to that of exogenous CoA, valinomycin-induced dissociation of [^{14}C]-CoA was significantly greater. Valinomycin or nigericin also caused efflux of endogenous CoA and, again, the effect of valinomycin was greater than that of nigericin. The results suggest that mitochondria contain a system that mediates net influx of CoA into the matrix. Further, the membrane electrical gradient is essential for the uptake and retention of CoA within the matrix. Supported by HL-37937.

Tu-Pos215

CONFORMATIONAL CHANGES OF MITOCHONDRIAL PRECURSOR PROTEINS AT VARIOUS STEPS ON THE IMPORT PATHWAY
Ilona S. Skerjanc and Gordon C. Shore (Intro. by Dr. D. MacLennan), Dept. of Biochem., McGill Univ., Mtl.,Can. H3G 1Y6

The conformation of two hybrid precursor proteins was examined at various points on the mitochondrial import pathway, by measuring precursor sensitivity to exogenous proteases and precursor specific enzymatic activity. We have found that they exhibit a near-native structure after synthesis in reticulocyte lysate, upon binding to liposomes, and upon binding to the surface of mitochondria. A mitochondrial translocation intermediate has been detected, the formation of which requires an intact signal sequence, a protease-sensitive component of the outer membrane, and ATP. It was found to have a negligible specific enzymatic activity and an increased susceptibility to trypsin compared to cytosolic precursor, suggesting that it had at least partially unfolded. Taken together, the results are consistent with a model in which the precursor protein unfolds as a consequence of engaging the mitochondrial translocation apparatus.

Tu-Pos216

IMPORT OF APOCYTOCHROME *c* INTO MITOCHONDRIA. T.B.M. Hakvoort, J.R. Sprinkle, and E. Margoliash. Dept. of Biochem. and Molecular Biology, Northwestern University, Evanston, Illinois 60208

Drosophila melanogaster apocytochrome *c*, made biosynthetically *in vitro* and purified to homogeneity in the monomeric state, shows two phases in its uptake by mouse liver mitochondria into a protease protected compartment of the organelle. The high affinity phase occurs only in the presence of a cell extract and saturates rapidly as the concentration of apocytochrome *c* is increased, while the low affinity phase is observed in the absence of the tissue factor and at higher concentrations of apoprotein in its presence. It does not saturate over a wide range of apocytochrome *c* concentrations, the uptake remaining proportional to the concentration of added apoprotein. This tissue factor was shown to be a protein. *In vitro* experiments with a large variety of site-directed mutants and constructs demonstrated that covalent binding of the apoprotein to heme is not required for the uptake mechanism, and that several segments in the central region (Residues 35-90) can substitute for each other. It was concluded that the high affinity uptake represents the normal physiological mechanism, while the low affinity phenomenon is the well studied melting of apocytochrome *c* through bilayer membranes. (NIH grants GM-19121 and GM-29001)